



The Assessment of Effects of Carbon Quantum Dots on Immune System Biomarkers Using  
RAW 264.7 Macrophage Cells

By

**Jodi Fowler**

A thesis submitted in fulfilment of the requirements for the degree of Magister Scientiae  
(M.Sc.) in Medical Bioscience (Immunology) in the Department of Medical Bioscience,  
University of the Western Cape, South Africa

Supervisor: Prof. E.J. Pool

Co-supervisor: Prof. M. Fidalgo

**December 2019**

## Declaration

I, **Jodi Fowler**, declare that the thesis entitled ‘**The Assessment of Effects of Carbon Quantum Dots on Immune System Biomarkers Using RAW 264.7 Macrophage Cells**’ is my work and has not been submitted for any degree or examination at any other university and that all sources of my information have been quoted as indicated in the text and/or list of reference.

Jodi Fowler

A handwritten signature in black ink that reads "Fowler". The letter "F" is large and stylized, with a vertical line extending downwards from its base. The rest of the name "owler" is written in a cursive, flowing script.

-----

Date:

## **Abstract**

Nanotechnology is a rapidly growing field of research. Due to major innovations brought about by developments in nanotech, several consumer products are currently available containing nanomaterials. The increase of nanomaterial production and use is accompanied by the increased potential of human, plant and animal exposure to these nanomaterials.

As a relatively new nanomaterial, carbon quantum dots (CQDs) are being extensively used and researched due to its unique properties. Although many studies have assessed the toxic potential of CQDs, and found them to exhibit low toxicity, there is lack of work assessing the effects on the immune system.

In the present study, RAW 264.7 murine macrophages were used as model to assess the immunomodulatory potential of CQDs. RAW cells exposed to varying concentrations of CQDs (0-500 $\mu$ g/ml), showed that CQDs caused a reduction at cell viability. In the absence of a mitogen CQDs, induced an inflammatory response by stimulating the release of various cytokines and chemokines such as, TNF $\alpha$ , MIP-1 $\alpha$ , MIP-1 $\beta$ , MIP-2, IP-10, G-CSF, GM-CSF, and JE.

## **Acknowledgements**

I wish to thank my supervisor, Prof. Edmund Pool, for his patience, guidance, and advice he has provided to me throughout my time as his student.

I would like to thank Prof. Maria Fidalgo and Mohamed Bayati from the University of Missouri for graciously providing the carbon quantum dots for this study.

I am grateful to the NRF, Ada Bertie Levenstein and Ethel and Erickson trust for their financial support during this research project

To my friends and lab mates, thank you for being there when I needed any assistance, lunch or some fresh air.

I would like to express my sincere gratitude to my family for their continuous love and support through all of the highs and lows of my research. A very special thank you to my favourite proof reader, my husband for always availing himself to read countless pages of edits. To my parents, I am forever indebted to you for affording me the best opportunities and experiences that have made me who I am. Thank you for always encouraging me to explore and always live life to the fullest. This journey would not have been possible if not for you, and I dedicate this milestone to you.

## List of Acronyms and Abbreviations

°C	Degrees Celsius
Ab	Antibodies
Ag	Antigen
AgNPs	Silver Nanoparticles
AlNPs	Aluminium Nanoparticles
ANOVA	Analysis of Variance
ATCC	American Type Culture Collection
Au	Gold
AuNPs	Gold Nanoparticles
B lymphocytes	Bone marrow-derived Lymphocytes
BLAF	Bronchoalveolar Lavage Fluid
C	Carbon
CeO <sub>2</sub>	Cerium Oxide
CNPs	Carbon Nanoparticles
CNTs	Carbon Nanotubes
CQDs	Carbon Quantum Dots

CO <sub>2</sub>	Carbon Dioxide
DAS-ELISA	Double Antigen Sandwich ELISA
DLS	Dynamic Light Scattering
DMEM	Dulbeccos Modified Eagle Medium
DNA	Deoxyribonucleic Acid
DPBS	Dulbeccos Phosphate Buffered Saline
DTA	Differential Thermal Analysis
ELISA	Enzyme-linked Immunosorbent Assay
FBS	Fetal Bovine Serum
FTIR	Fourier-transform Infrared Spectroscopy
G-CSF	Granulocyte-colony Stimulating Factor
GIT	Gastrointestinal Tract
GM-CSF	Granulocyte-macrophage Colony-stimulating Factor
HSA	Human Serum Albumin
ICP-AES	Inductively Coupled Plasma Atomic Emission Spectroscopy
IEP	Isoelectric Point
IFN $\gamma$	Interferon Gamma
Ig	Immunoglobulin

IgE	Immunoglobulin E
IgG	Immunoglobulin G
IgM	Immunoglobulin M
IL-1ra	Interleukin 1 Receptor Agonist
IL-1 $\beta$	Interleukin-1 beta
IL-6	Interleukin-6
IL-27	Interleukin-27
IP-10	IFN $\gamma$ -inducible Protein-10
JE	Monocyte Chemoattractant Protein 1
LPS	Lipopolysaccharide
MIP-1 $\alpha$	Macrophage Inflammatory Protein 1 alpha
MIP-1 $\beta$	Macrophage Inflammatory Protein 1 beta
MIP-2	Macrophage Inflammatory Protein 2
MRI	Magnetic Resonance Imaging
NaCl	Sodium Chloride
NK	Natural Killer cells
NO	Nitric Oxide

nm	Nanometers
NP	Nanoparticle
PBS	Phosphate Buffered Saline
PEG	Polyethylene Glycol
pg/ml	Picograms per Millilitre
QDs	Quantum Dots
ROS	Reactive Oxygen Species
SEM	Scanning Electron Microscopy
SD	Standard Deviation
SDF-1	Stromal cell-derived factor 1
SSA	Specific Surface Area
SWCNTs	Single Walled Carbon Nanotubes
Tc	Cytotoxic Thymus- lymphocytes
Th1	Thymus- Helper type 1 lymphocytes
T lymphocytes	Thymus Lymphocytes
TEM	Transmission Electron Microscopy
TiO <sub>2</sub>	Titanium Dioxide



TiO <sub>2</sub> NP	Titanium Dioxide Nanoparticles
TMB	Tetramethylbenzidine
TNF- $\alpha$	Tumour Necrosis Factor Alpha
UFP	Ultrafine Particles
UV-Vis	Ultraviolet-visible Spectroscopy
$\mu\text{g/ml}$	Micrograms per Milliliter
v/v	Volume per Volume
WST-1	Water Tetrazolium Salt
w/v	Weight per Volume
XPS	X-ray Photoelectric Spectroscopy
XRD	X-ray Diffraction

## Research Papers and Poster Presentations at Conferences

- Lategan, K., Leach, L., Alghadi, H., Fowler, J., Fidalgo, M. and Pool, E. (2017) The use of proteome profiling to detect potential biomarkers for monitoring the immunotoxicity of engineered nanoparticles. SETAC Europe, Brussels, Belgium, 7-11 May 2017
- Lategan, K., Fowler, J., Bayati, M., Fidalgo de Cortalezzi, M. and Pool, E. (2018) The Effects of Carbon Dots on Immune System Biomarkers, Using the Murine Macrophage Cell Line RAW 264.7 and Human Whole Blood Cell Cultures. *Nanomaterials (Basel)*, 8(6)

## List of Figures

**Figure 4.1.** Visualization of carbon quantum dots via transmission electron microscopy (TEM).

**Figure 4.2.** Zeta potential of carbon quantum dots under varying pH levels, while maintaining a constant ion concentration of 10 mM NaCl.

**Figure 5.1.** Cell viability of RAW 264.7 cells exposed to CQDs. The results are presented as mean  $\pm$  SD with  $n = 9$ . Significance demarcated by: a- significantly different ( $P < 0.001$ ) compared to 0  $\mu\text{g/ml}$  CQD control.

**Figure 5.2.** NO levels of RAW 264.7 cell cultures exposed to CQDs. The results are presented as mean  $\pm$  SD with  $n = 9$ . Significance demarcated by: a- significantly different ( $P < 0.001$ ) compared to the 0  $\mu\text{g/ml}$  CQD control.

**Figure 5.3.** IL-6 levels of unstimulated RAW 264.7 cell cultures exposed to CQDs. The results are presented as mean  $\pm$  SD with  $n = 9$ . Positive control (+ LPS) not presented ( $56\,748 \pm 9\,591.8$  pg/ml IL-6). Significance demarcated by: a- significantly different ( $P < 0.001$ ) compared to 0  $\mu\text{g/ml}$  CQD control.

**Figure 5.4.** MIP-1 $\alpha$  levels of unstimulated RAW 264.7 cell cultures exposed to CQDs. The results are presented as mean  $\pm$  SD with  $n = 9$ . Positive control (+ LPS) not presented ( $1\,637\,093 \pm 199\,883.8$  pg/ml MIP-1 $\alpha$ ). Significance demarcated by: a- significantly different ( $P < 0.002$ ) compared to 0  $\mu\text{g/ml}$  CQD control.

**Figure 5.5.** MIP-1 $\beta$  levels of unstimulated RAW 264.7 cell cultures exposed to CQDs. The results are presented as mean  $\pm$  SD with  $n = 9$ . Positive control (+ LPS) not presented ( $343\,965 \pm 52\,044$

pg/ml MIP-1 $\beta$ ). Significance demarcated by: a- significantly different ( $P < 0.001$ ) compared to 0  $\mu\text{g/ml}$  CQD control.

**Figure 5.6.** MIP-2 levels of unstimulated RAW 264.7 cell cultures exposed to CQDs. The results are presented as mean  $\pm$  SD with  $n = 9$ . Positive control (+ LPS) not presented ( $302\,089 \pm 68\,868$  pg/ml MIP-2). Significance demarcated by: a- significantly different ( $P < 0.001$ ) compared to 0  $\mu\text{g/ml}$  CQD control.

**Figure 5.7.** The effect of CQDs on RAW 264.7 cells. Cells were incubated with (a) culture media only (negative control), (b) LPS-stimulated media (positive control) and (c) 500  $\mu\text{g/ml}$  CQDs in the absence of LPS. Supernatants were assayed using the proteome profiler array as described in the methods section. Cytokines/chemokines that were detected were allocated numbers: 1, 3, and 16 are reference spots, 2- IP-10; 4- G-CSF; 5- TNF- $\alpha$ ; 6- GM-CSF; 7- IL-6; 8- JE; 9-ICAM-1; 10- MIP-1 $\alpha$ ; 11- MIP-1 $\beta$ ; 12- IL-1 $\beta$ ; 13- MIP-2; 14- IL-1ra; 15- RANTES; 17- IL-27; 18-SDF-1.

## List of Tables

**Table 2.1.** A summary of the characterization tools for NPs (Chen et al., 2010, Dhawan and Sharma 2010, Li et al., 2009, Sayes and Warheit 2009, Tien et al., 2008)

**Table 5.1.** The effects of CQDs on RAW 264.7 cells expression of chemokines and cytokines. Cells not stimulated with LPS after treatment with medium only (negative control), medium containing LPS (positive control) or medium containing 500 µg/ml CQDs. Membranes were subjected to chromogenic exposure. ‘Yes’ represents the presence while ‘No’ represents the absence of cytokines and chemokines in response to the exposures, to the naked eye.

## Table of Contents

<b>Declaration</b> .....	ii
<b>Abstract</b> .....	iii
<b>Acknowledgements</b> .....	iv
<b>List of Acronyms and Abbreviations</b> .....	v
<b>Research Papers and Poster Presentations at Conferences</b> .....	x
<b>List of Figures</b> .....	xi
<b>List of Tables</b> .....	xiii
<b>Table of Contents</b> .....	xiv
<b>Chapter 1:</b> .....	1
<b>Introduction</b> .....	1
<b>Chapter 2:</b> .....	4
<b>Literature Review</b> .....	4
<b>2.1. Background</b> .....	4
<b>2.2. Properties of Nanoparticles</b> .....	4
<b>2.3. Synthesis</b> .....	6
2.3.1. Top-down Approach for Nanoparticle Synthesis.....	7
2.3.2. Bottom-up Approach for Nanoparticle Synthesis .....	7
<b>2.4. Post-synthesis Processing of Nanoparticles</b> .....	8
2.4.1. Purification of Nanoparticles .....	8
2.4.2. Surface Passivation and Functionalization of Nanoparticles .....	8
<b>2.5. Characterization of Nanoparticles</b> .....	9
<b>Chapter 3:</b> .....	11
<b>Nanotoxicology</b> .....	11
<b>3.1. Factors Affecting Nanotoxicity</b> .....	12
<b>3.2. Routes of Exposure</b> .....	12
<b>3.3. Immunotoxicity</b> .....	16
<b>3.4. Carbon Quantum Dots (CQDs)</b> .....	20
<b>3.5. Aim of this study</b> .....	24
<b>3.6. Hypothesis</b> .....	25
<b>Chapter 4:</b> .....	26
<b>Methods</b> .....	26
<b>4.1. Nanoparticle Synthesis</b> .....	26
<b>4.2. Nanoparticle Preparation</b> .....	27

<b>4.3. Cell Culture Reagents</b> .....	27
<b>4.4. Cells Exposure to CQDs</b> .....	28
<b>4.5. Cell Viability</b> .....	29
<b>4.6. Nitric Oxide (NO)</b> .....	29
<b>4.7. Interleukin 6 (IL-6)</b> .....	30
<b>4.8. Murine MIPs (MIP-1<math>\alpha</math>, MIP-1<math>\beta</math> and MIP-2) ELISAs</b> .....	30
<b>4.9. Murine Cytokine Proteome Profiling Array</b> .....	31
<b>4.10. Quantification of Pixel Density for Cytokine Blot</b> .....	32
<b>4.11. Statistical Analysis</b> .....	32
<b>Chapter 5:</b> .....	33
<b>Results</b> .....	33
<b>5.1. The Effects of CQDs on RAW 264.7 Cell Viability</b> .....	33
<b>5.2. The Effects of CQDs on the Inflammatory Biomarker NO Secretion by RAW 264.7 Cells</b> ...	34
<b>5.3. The Effects of CQDs on the Inflammatory Biomarker IL-6 Secretion Using RAW 264.7 Cells</b> .....	34
<b>5.4. The Effects of CQDs on Chemokines Secretion Using RAW 264.7 Cells</b> .....	35
5.4.1. The Effects of CQDs on MIP-1 $\alpha$ Secretion Using RAW 264.7 Cells .....	35
5.4.2. The Effects of CQDs on MIP-1 $\beta$ Secretion Using RAW 264.7 Cells .....	36
5.4.3. The Effects of CQDs on MIP-2 Secretion Using RAW 264.7 Cells .....	37
<b>5.5. The Effects of CQDs on the Secretory Cytokine and Chemokine Profile of RAW 264.7 Cells</b> .....	38
<b>Chapter 6:</b> .....	42
<b>Discussion</b> .....	42
<b>Chapter 7:</b> .....	47
<b>Conclusion and Future Perspectives</b> .....	47
<b>7.1. Conclusion</b> .....	47
<b>7.2. Future Perspectives</b> .....	47
<b>References</b> .....	49

## **Chapter 1:**

### **Introduction**

In the last twenty to thirty years, nanotechnology has been extensively researched. This is due to the characteristic small size of nanoparticles (NPs), imparting nanomaterials with properties that are different to that of their bulk counterparts. Nanoparticles have at least one dimension in the size range of 1-100nm (Bayati et al., 2017). Because of their small size NPs have an increased surface area to volume ratio, allowing higher surface reactivity and different physico-chemical properties compared to their bulk counterparts (Yildirimer et al., 2011). These properties allow NPs to be manipulated for various applications and they are thus being increasingly used to replace bulk particles (Armstead and Li 2016).

Nanoparticles have been shown to have applications in biomedicine, materials manufacturing, electronics, energy harvesting, and mechanical industries (Donaldson et al., 2004, Khan et al., 2017). With increased usage in these industries, there is an increased risk of NPs entering the environment, resulting in human, animal and plant exposures (Agarwal et al., 2013, Donaldson et al., 2004).

Common routes of NP human exposure are dermal exposure through NPs found in sunblock or other cosmetic products, ingestion of NPs in foods and medication, injections of NPs for therapeutics and diagnostics, or inhalation of NPs through, medication, industrial and manufacturing procedures (Donaldson et al., 2004, Khan et al., 2017).



Although NPs have generally been proposed to produce breakthrough applications, their small size may pose adverse effects as they may be able to pass through barriers or interact with vital organ systems that may be impossible for bulk materials (Agarwal et al., 2013, Yildirimer et al., 2011). This has led to the field of study called nanotoxicology, which is aimed at investigating the potential adverse effects of NPs (Agarwal et al., 2013, Donaldson et al., 2004).

Nanotoxicity can be described as a change in normal physiological functions following exposure to NPs (Fu et al., 2014). Several groups have utilized *in vivo* and *in vitro* studies to identify the potential toxic effects of NPs on organ systems and have determined that NPs can cause granuloma formations in the lungs, induce deoxyribonucleic acid (DNA) damage, generate reactive oxygen species (ROS) and reduce cell viability (Agarwal et al., 2013, Yildirimer et al., 2011).

One important system that NPs interact with is the immune system. This is due to immune cells constantly guarding against foreign invaders in order to maintain homeostasis by eradicating any foreign invaders (Kononenko et al., 2015). As foreign materials, NPs are encountered by immune cells and NPs thus have the potential to alter immune functions, inducing a state called immunotoxicity, which is undesirable as it may leave the host susceptible to illness. It is thus imperative to evaluate the immunotoxic potential of NPs before they are used commercially (Kononenko et al., 2015).

Carbon quantum dots (CQDs), a relatively new nanoparticle discovered in 2004 has been highly researched due its low toxicity, solubility, biocompatibility and fluorescent properties, allowing CQDs to employed as a replacement for heavy metal semiconductor quantum dots (Bayati et al., 2017). As an implication of its incorporation into several applications, CQD production is increasing, ultimately leading to increased probability of human exposure. To our

knowledge only one paper has been published relating to the immunomodulatory effects of CQDs, using an *in vivo* study (Gao et al., 2013). No studies have investigated the immunomodulatory effects of CQDs on RAW 246.7 macrophages. There is thus a gap in the academic literature which we aim to investigate. For CQDs to effectively replace semiconductor quantum dots they must be safer and cheaper to produce than the heavy metals currently used (Wang and Hu 2014). We therefore propose the evaluation of CQDs synthesized via a cost-effective method. The produced CQDs effects will be evaluated using RAW 264.7 macrophages as macrophages are one of the first cells to detect and eradicate foreign material to return the body to homeostasis (Kononenko et al., 2015).

## **Chapter 2:**

### **Literature Review**

#### **2.1. Background**

Nanoparticles (NPs) are small particles which ranges in size from 1nm to 100nm (Huang and El-Sayed 2010). Nanoparticles can be synthesized in laboratories or they may occur naturally as a result of environmental processes such as weathering, volcanic eruptions, wildfires or microbial processes (Heiligtag and Niederberger 2013). They have existed for many years before they became popular and the most prominent discovery was the use of nanoparticles as colour pigments for ceramics. Nanoparticles differ significantly from bulk particles because they are much smaller and have a greater surface area, thus replacing bulk materials with NPs has the potential to alter the functionality of materials (Burda et al., 2005). Common properties that are changed at the nano-scale include: material strength, lighter weight, increased control of light spectrum, and greater chemical reactivity due to NPs having an increased surface area to volume ratio when compared to bulk particles (Liu 2006). Because of the altered properties of materials at the nano-scale, NPs have been incorporated into various applications in several disciplines such as science (physical, chemical, biological and environmental), pharmacy, medicine, electronics, and communications (Mohanraj and Chen 2006, Zoroddu et al., 2014)

#### **2.2. Properties of Nanoparticles**

Nanoparticles are of great scientific importance because they provide a link to aid the understanding between bulk materials and molecular or atomic structures (Burda et al., 2005). Bulk materials have constant physical properties regardless of their size while their properties change as the size of materials approaches the nano-scale range. The properties of materials change

as they become smaller and this is due to the increase of particles at the surface of the material (Elsaesser and Howard 2012, Huang and El-Sayed 2010). Properties such as particle size, surface area, surface charge, shape/structure, solubility, and surface coatings are known to affect the applications of NPs in several industries (Sayes and Warheit 2009, Schmid and Corain 2003, Zoroddu et al., 2014). The optical properties of nanoparticles differ significantly from bulk materials because nanoparticles are small enough to restrict their electrons, resulting in quantum effects. Bulk gold (Au) particles appear shiny yellow while gold nanoparticles (AuNPs) are never shiny but instead appear deep red to black (Schmid and Corain 2003). The difference in colour observation between bulk materials and NPs is due to NPs absorbing light at one wavelength and releasing their energy, by emitting light at another wavelength (Huang and El-Sayed 2010). The colour of the emitted light is dependent on the size of the particle, when light excites a larger particle the colour that is observed is redder, however, the excitation of a smaller particle results in a bluer colour (Huang and El-Sayed 2010). Many other properties such as catalytic activity, melting point, surface reactivity and conductivity, change as materials reach the nano-scale range (Burda et al., 2005, Utekhina and Sergeev 2011). An example of this change in physical properties occurs when their melting point decreases as the size of the material decreases. This phenomenon is referred to as the melting-point depression. The melting point of bulk Au particles is Au (1064 °C) while the melting point of AuNPs is approximately 300 °C for 2.5 nm size, and this can differ based on the size of the nanoparticle (Schmid and Corain 2003). As previously mentioned, NPs have a larger surface area to volume ratio compared to bulk materials. This allows for an increase in the number of atoms exposed at the surface of the nanomaterials, which in turn increases the number of sites where potential reactions may occur, increasing the reactivity of NPs compared to their larger sized particles of the same material (Burda et al., 2005).

### **2.3. Synthesis of Nanoparticles**

Since several NPs exist, it has become necessary to classify NPs. One method is to categorise NPs based on their route of synthesis. Thus, nanoparticles can be classified as either engineered or as naturally occurring. Naturally occurring nanoparticles can also be defined as ultrafine particles (UFP) and these materials are synthesized during everyday activities, environmental occurrences or during industrial procedures as by-products (Chang 2010). They can further be classified as anthropogenic which are produced as a result of human activities such as tobacco smoke or diesel burning, or naturally occurring which are those produced because of naturally occurring environmental processes: weathering, volcanic eruptions, magneto-tactic bacteria, ocean spray, wildfires and microbial processes (Chang 2010, Heiligtag and Niederberger 2013).

On the other hand, engineered NPs are those which are synthesized for specific applications (Chang 2010). It is preferred to use engineered NPs in applications as opposed to naturally occurring NPs because engineered NPs can be designed for the intended application which relies on specific properties and can only be achieved via the highly controlled synthesis of the NPs (Allouche 2013, Heiligtag and Niederberger 2013).

Engineered NPs can be synthesized via two approaches, top-down and bottom-up (Yadav et al., 2012). During top-down processes, large materials are chemically or mechanically broken down to produce smaller particles, while nanoparticles produced by bottom-up processes are formed by the self-assembly of atoms and molecules. Both procedures can be done in either gas, liquid, supercritical fluids, solid states, or in vacuum (Yadav et al., 2012).

### 2.3.1. Top-down Approach for Nanoparticle Synthesis

During top-down processes, nanoparticles are produced by the physical disintegration of larger solid materials or chemical processing. Top-down processes produce nano-scaled structures using shear forces such as compression, friction, and shock or using a milling apparatus (Pal et al., 2010). The methods most commonly implemented include milling, arc-discharge method, lithography and laser ablation. Top-down procedures are often expensive as specialized machines and tools are required for NP production (Utekhina and Sergeev 2011).

### 2.3.2. Bottom-up Approach for Nanoparticle Synthesis

As opposed to top-down procedures, bottom-up methods do not require expensive apparatus. The bottom-up method can be divided into gaseous and liquid phase reactions. During gaseous phase reactions, a solid is heated to the point where it becomes evaporated into background gas, to achieve supersaturation. Supersaturation is highly important as it promotes crystal nucleation and growth of the NPs (Swihart 2003).

Several methods exist for nanoparticle synthesis. The synthetic method employed depends on the specific properties required for the applications of the intended nanoparticle.

Factors such as particle size, impurities, aggregation, shape, crystal structure and reactant structure impacts the functions of NPs. These properties can be altered by changing the duration of synthesis, temperature, wavelength or precursors (Arbain et al., 2011, Chen and He 2001, Chen et al., 2010, Tani et al., 2002, Tsuji et al., 2002)

## **2.4. Post-synthesis Processing of Nanoparticles**

### **2.4.1. Purification of Nanoparticles**

Nanoparticles are often produced non-uniformly and the resultant NPs are of various shapes and sizes. Lack of uniformity poses a problem, as the functions of nanoparticles are related to the size and shape, thus produced NPs may have different functions. Therefore, the size and shape of all the produced particles need to be consistent (Wang and Hu 2014). Uniformity can be achieved via post-treatment methods such as filtration, centrifugation, and column chromatography and gel electrophoresis which allows for the isolation of the intended NPs (Mori 2015, Wang and Hu 2014).

### **2.4.2. Surface Passivation and Functionalization of Nanoparticles**

Nanoparticles are extremely sensitive to contamination as it may lead to a change in the properties of the NP's surface and this could alter the functionality of the NPs. It is for this reason that the surface of the NPs should be modified to maintain the integrity of the NPs. This type of modification of NPs is referred to as passivation, which is employed to prevent highly reactive or aggregative NPs from being contaminated (Weingart et al., 2013). Biomedical NPs are often coated with various structures to prevent them from being removed by the immune system. This is due to NPs being recognised as foreign by the immune system, which in turn causes various protein including opsonins in the blood to bind to the NP's surface, forming a protein corona which signals the NP for eradication by immune cells. The NPs are thus prevented from performing their function within the body (Boraschi et al., 2012). One commonly used NP surface coat is polyethylene glycol (PEG), the process of coating a NP with PEG is known as 'PEGylation', this helps increase the NPs presence in circulation by evading the immune system (Suk et al., 2016)

Functionalization is commonly used in nanoparticle modification and is employed to commit a NP to a specific function such as a molecular recognition or fluorescence, to name a few functions (Weingart et al., 2013). In some instances, the passivating agents can also serve as a functionalization agent, where the physical properties of the NP are altered together with the functional properties. This allows for the NP to undergo less processing, which in turn reduces the possibilities for potential contamination in addition to reducing cost (Wang and Hu 2014). This was observed where the passivation of AuNPs using  $\omega$ -carboxy- and  $\omega$ -amino-polyethylene glycol (PEG) thiols, and carbon (C) with hyper-branched PEG. These passivation's resulted in AuNPs having increased binding specificity and carbon nanoparticles (CNPs) having increased fluorescence, respectively (Maus et al., 2010).

## **2.5. Characterization of Nanoparticles**

Following the synthesis of nanomaterials, it becomes necessary to determine if the particles produced exhibit the desired properties. The process of determining the properties of NPs is called, characterization. During characterization, the properties of nanomaterials (shape, size, surface chemistry and reactivity, solubility and chemical composition) are measured (Khan et al., 2017). Table 2.1. Presents short summary of the methods commonly used for NP characterization. Knowledge regarding the characteristics of NPs provides vital insights into understanding how NPs may react or interact in various environments.



**Table 2.1.** A summary of the characterization tools for NPs (Chen et al., 2010, Dhawan and Sharma 2010, Li et al., 2009, Sayes and Warheit 2009, Tien et al., 2008)

<b>Property</b>	<b>Definition</b>	<b>Technique</b>
<b>Particle size distribution (PSD)</b>	The range of sizes of particles within a sample. These measurements give an indication of the aggregation/agglomeration state	Dry <ul style="list-style-type: none"> <li>Scanning and transmission electron microscopy (SEM and TEM)</li> <li>Specific surface area (SSA)</li> <li>X-ray powder diffraction (XRD)</li> </ul> In suspension <ul style="list-style-type: none"> <li>Dynamic light scattering (DLS) is employed in aqueous phase</li> </ul>
<b>Particle morphology</b>	Shape (rod, spherical, filamentous)	Scanning and Transmission Electron microscopy (TEM and SEM)
<b>Chemical Composition</b>	Refers to the elements of which the material is composed Information on the material's intrinsic chemical toxicity can be attained Includes both composition of the particle's core and its surface	X-ray photoelectric spectroscopy (XPS) Raman spectroscopy Inductively coupled plasma atomic emission spectroscopy (ICP-AES) Differential thermal analysis (DTA) X-ray diffraction (XRD) Ultraviolet-visible spectroscopy (UV-Vis) Fourier-transform infrared spectroscopy (FTIR)
<b>Solubility</b>	A measure of how much of a given material will dissolve in a liquid Determines hydrophobicity, hydrophilicity, and lipophilicity	Visual conformation over time Conductance measurements
<b>Surface chemistry and reactivity</b>	The chemistry associated with surface of a material Information on the liquid -solid interface can be attained Often requires more than one test to characterize Surface charge is a useful measurement	Photodegradation of aqueous Congo Red Zeta potential Isoelectric point (IEP) Vitamin C assay Hemolytic potential X-ray photoelectric spectroscopy (XPS) Fourier-transform infrared spectroscopy (FTIR)

## **Chapter 3:**

### **Nanotoxicology**

Nanotoxicology is a relatively new field of study that developed long after NPs were used in the manufacturing of consumer products (Donaldson et al., 2004). The goal of this field is to assess the potential adverse effects of NPs. It has become necessary to evaluate the potential adverse effects of NPs because production of NPs in various disciplines is increasing, and with it, the potential risk of exposure through either voluntary or involuntary routes (Oberdörster et al., 2005). Unlike their bulk counterparts, NPs have a higher surface area to volume ratio, making them more reactive than bulk chemicals (Arora et al., 2012). Due to their increased reactivity, NPs can interact with various components and it is therefore necessary to understand how NPs will respond in different conditions. Thus, preliminary tests which replicate the intended environment of NPs are vital as NPs are not present in isolation, and these tests allow for the discovery of undesirable effects and improvement of the NPs before being used commercially (Arora et al., 2012).

The size-dependent properties of NPs which allow it to be exploited in various disciplines, are the very properties that could also result in adverse effects to humans and the environment. This is due to NPs being small enough to evade the body's barriers, and possibly enter the body via permeation through the skin, ingestion, inhalation or injection (Arora et al., 2012, Elsaesser and Howard 2012, Oberdörster et al., 2005, Zoroddu et al., 2014). Owing to their small size, NPs can translocate from the site of entry and move into the blood stream, allowing a passage for NPs throughout the body. Once in the blood stream, NPs can enter various organ systems and where they may potentially accumulate, causing altered functioning of those organs (De Jong and Borm 2008, Vishwakarma et al., 2010).

### **3.1. Factors Affecting Nanotoxicity**

As previously mentioned, the specific properties responsible for all NPs unique functionality are often also responsible for their adverse effects. The characteristics which play a role in nanotoxicity include size because smaller sized NPs have a larger surface area and more reactive sites. Their small size also allows NPs to cross the blood-brain barrier (Arora et al., 2012, Zoroddu et al., 2014). The shape and surface charge influence how NPs interact with cells and cellular components (Havrdova et al., 2016). The composition and surface coating also play a role in nanotoxicity as some potentially dangerous therapeutics are often coated to go unnoticed by the immune cells (Arora et al., 2012, Dhawan and Sharma 2010, Elsaesser and Howard 2012, Sayes and Warneit 2009, Zoroddu et al., 2014).

### **3.2. Routes of Exposure**

The most common entry for airborne NPs into the body occurs via inhalation (Yang et al., 2008). Inhalation provides a direct pathway for NPs to enter the respiratory system through the nasal passage. NP inhalation often occurs as a result of by-products from industrial processes which may be released into the environment and ultimately are inhaled by individuals via the occupational exposure of workers in these industrial fields (Elsaesser and Howard 2012, Santos and Vieira 2017, Zoroddu et al., 2014). This was observed where individuals had aluminium NPs in their lungs following exposure to surfaces coated with aluminium NPs (Santos and Vieira 2017). Nanoparticles can also be inhaled intentionally as part of an alternative treatment to oral administration, especially for proteins or poorly water-soluble drugs that have low bioavailability via the oral route (Yang et al., 2008). Once inhaled, larger particles are deposited in the nose, mouth and larynx, whereas the smaller particles can reach the bronchial tree and may be retained where they may exert potentially dangerous effects during respiration

(Srinivasa et al., 2011). Inhaled NPs can also gain access to other organs via the olfactory bulb, where they are able to translocate to the central nervous system (Liu et al., 2009). Rat studies by Sung et al (2008) and Srinivasa et al (2011) evaluated the outcome following inhalation of silver nanoparticles (AgNPs) and cerium oxide nanoparticles (CeO<sub>2</sub>), respectively. Following exposure to AgNPs, a dose- and time-dependent increase in AgNPs concentration was observed along with correlating increases in alveolar inflammation and a small granulomatous lesion. Cerium oxide NPs caused the induction of pro-inflammatory cytokines which in turn stimulated oxidative stress, lipid peroxidation, increased microvascular permeability and cell lysis in lung epithelium. Cerium oxide NPs were also found to enter alveolar, bronchi and bronchiole region within the first 24 hours post exposure (Srinivasa et al., 2011).

Inhalation of NPs have also been assessed for their role in cancer by Hong et al (2017). In the study, ICR (CD-1) male mice were exposed to titanium oxide nanoparticles (TiO<sub>2</sub>) at various concentrations (0, 1.25, 2.5, or 5 mg/kg body weight), daily for 9 months. The TiO<sub>2</sub> NPs caused infiltration of inflammatory cells and tumorigenesis in the lung. The NPs caused significant increases of lactate dehydrogenase, alkaline phosphatase, and total protein levels in bronchoalveolar lavage fluid (BLAF). There were also significant increases in tumor markers including cytokeratin 19, neuron-specific enolase, carcinoembryonic antigen, squamous cell carcinoma antigen, and cancer antigen-125 in the serum. Hong and associates (2017) concluded that further studies were needed to determine the effects of long-term exposure to NPs.

Apart from *in vivo* studies, the effects of NPs on the respiratory system can also be assessed using *in vitro* methods. *In vitro* studies assessing silica NPs and single walled carbon nanotubes (SWCNTs) have shown reduced cell viability of lung cancer cell lines following NP exposure

(Davoren et al., 2007, Lin et al., 2006). Napierska et al (2009) found that smaller silica NPs (particle size < 100nm) caused a greater reduction in cell viability than those above 100nm.

As the largest organ of the body, the purpose of the skin is to provide a direct barrier against the external environment and it is thus exposed to several toxins, such as NPs in the environment (Elsaesser and Howard 2012). Intentional dermal exposure of NPs is common due to NPs being incorporated into various cosmetic products such as shampoo, toothpaste, deodorant, soap, sunscreen, cream, perfumes and make-up. Intentional usage of products containing NPs allows for direct application of these NPs, allowing these particles to penetrate the surface of the skin (Zoroddu et al., 2014). In healthy, undamaged skin, penetration is most likely along two possible routes: the intercellular route, following the lipid channels between the corneocytes to deeper skin layers or via hair follicles and sweat glands (Schneider et al., 2009). Titanium dioxide nanoparticles (TiO<sub>2</sub> NPs) are often incorporated into sunscreen products and may gain access through hair follicles, wounds or lesions (Weir et al., 2012). The cytotoxic effects of silica and TiO<sub>2</sub> NPs were assessed in two separate studies on the human dermal keratinocyte cell line (HaCat). Viability of HaCat cells were reduced in a dose- dependent manner in response to both NPs (Liang et al., 2013, Wright et al., 2017). Another study using Langerhans cells showed that smaller silica NPs were both taken up faster and more toxic than larger sized particles (Nabeshi et al., 2010). In SK-Mel-28, the highest level of cytotoxicity caused by AuNPs was seen with smaller NPs (1.4 nm) (Pan et al., 2007).

Nanoparticle exposure can also occur through ingestion. Due to the size specific properties, NPs have been incorporated into various food products to improve packaging, gaseous and microbial detection or to enrich the food with important vitamins and preservatives (Duncan 2011, He and Hwang 2016, Mills and Hazafy 2008, Peters et al., 2011). In addition to NPs being

ingested in food, NPs can also be ingested via water sources contaminated with NPs. Once ingested, NPs enter the gastrointestinal system (GIT) where they could gain access to the blood stream via gastro-intestinal assimilation and enter other organs. A study by Jani et al (1990), showed that when polystyrene microspheres ranging from 50nm to 3 microns were fed to mice, smaller NPs (50nm) showed higher levels of absorption and translocation to other organs such as liver, spleen, blood and bone marrow compared to larger NPs. Particles larger than 100 nm did not reach the bone marrow, and those larger than 300 nm were absent from blood. This indicates that the size and morphological properties of NPs influence their absorption from the gastrointestinal area. The absorption is greater for the smaller than for the larger particles (Zoroddu et al., 2014).

As a component of many therapeutics, NP exposure can occur through injections. Advances in nanotechnology have identified an array of NPs for biological and biomedical applications due to their small particle size, novel physicochemical properties, and easy surface modification (Cho et al., 2009a). Nanoparticles have been proposed to protect drugs from the body's protective systems, which are often responsible for degrading and removing drugs before they are able to interact with their target (De Jong and Borm 2008). Nanoparticles in biomedicine and biology have also been utilized in fluorescent biological labels for diagnostics, bio-detection of pathogens and proteins, probing of DNA structure, tissue engineering, tumour destruction via heating (hyperthermia), separation and purification of biological molecules and cells and magnetic resonance imaging (MRI) contrast enhancement (Salata 2004). Through biomedicine, NPs are directly injected into the bloodstream which allows NPs to directly interact with cells and organs of the body where they may accumulate and cause potential detrimental effects. Cho et al (2009b) injected BALB/C mice with AuNPs and found AuNPs accumulated in the liver and spleen in addition to causing upregulation of inflammatory cytokines (IL-1, 6, 10 and TNF- $\alpha$ ) and apoptosis

of hepatocytes at the highest concentrations (4.26 mg/kg) (Cho et al., 2009b). Inflammation was also observed after the injection of silica NPs in BALB/C mice, in addition to NP size-dependent hepatic toxicity (Cho et al., 2009a). However, injection of mice with silica NPs of a smaller size and at a lower concentration showed higher accumulation of silica NPs in liver, spleen and intestines but no pathological changes were observed with small NP (< 25 nm) (Kumar et al., 2010).

As shown above, NPs can interact with and cause potentially detrimental effects to various parts of the body. The effects that NPs may cause depend on the properties of the NP and the environment in which the NPs are present in (Gatoo et al., 2014).

### **3.3. Immunotoxicity**

The primary function of the immune system is to protect the body against foreign matter. However, certain conditions prevent the immune system from performing efficiently, inducing a state of immune dysfunction, referred to as ‘immunotoxicity’ (National Research Council 1992). The multi-disciplinary field of study investigating immunotoxicity is called immunotoxicology, which incorporates various fields such as immunology and toxicology (Germolec et al., 2017, Konig 2011).

Immunotoxicity arises following exposure to chemical and physical agents that hinder the capability of the immune system. Foreign agents responsible for causing immune dysfunction are called xenobiotics (Descotes 2005, Konig 2011). Xenobiotics may be artificially synthesized compounds or naturally occurring elements and compounds in the environment (Donner et al., 2010). Xenobiotics can either be physical or chemical agents. The exposure to chemical xenobiotics can be of either an environmental or occupational origin such as:

insecticides, herbicides, polycyclic aromatic hydrocarbons, halogenated hydrocarbons, and heavy metals. Chemical xenobiotics can also be introduced as pharmaceuticals such as: corticosteroids, cyclosporine, cyclophosphamide, and methotrexate, or drugs such as: alcohol, tobacco, opioids, and cannabinoids (Konig 2011, Kuricova et al., 2012). Physical agents that cause immunotoxicity, include ultraviolet light and ionizing radiation (Konig 2011).

The effects caused by xenobiotics rely on the mode and the duration of xenobiotic exposure (Kreitinger et al., 2016). Individuals may be introduced to xenobiotics via inhalation, ingestion, dermal contact and injection (circulation/muscles) (Kononenko et al., 2015, Kreitinger et al., 2016). The effects of xenobiotics also depend on its physico-chemical properties such as: solubility, chemical reactivity, and size. Other factors that determine the impact of xenobiotics include the concentration of the chemical, as well as pre-existing medical issues of the exposed individual. Thus, everyone may not respond the same to the same xenobiotics (Kononenko et al., 2015).

When mammals are exposed to xenobiotics, xenobiotics are first encountered by innate immune cells (phagocytes and humoral factors) (Boraschi et al., 2017). Following detection by a fully functioning immune system, xenobiotics are eradicated via phagocytosis and the break down products are used to form antibodies (Abs) which remains present for faster resolution should the xenobiotic re-enter the body (Boraschi et al., 2017).

When a xenobiotic induces immune dysregulation, immunotoxic effects can manifest as immunosuppression, immunostimulation, hypersensitivity and autoimmunity (Descotes 2005, Konig 2011).



Immunosuppression results in reduction or absence of immune responses. Immune organs or immune cells may not be properly developed or may be present, but in lowered amounts. This prevents the body from having the ability to adequately fight pathogens (Konig 2011). Immunosuppression renders the body susceptible to many infections and cancer (Shevach 2009). Immunosuppression is often induced following the use of immunosuppressive drugs for the success of organ transplants or by other chemicals which may influence the number of immune cells (De Jong and Van Loveren 2007). Often, immunosuppressive drugs and xenobiotics lead to immunodeficiency, which reduces the body's resistance to various pathogens, resulting in various illnesses (De Jong and Van Loveren 2007, Shevach 2009).

Immunostimulation is the opposite of immunosuppression and promotes increased immune responses. This dysregulation of the immune system results in the induction of immune responses, regardless of whether it is intended or not (De Jong and Van Loveren 2007). This overstimulation of immune responses may lead to chronic inflammation which has been implicated as a major contributor in many chronic diseases (Konig 2011).

Hypersensitivity occurs when the immune system elicits an exaggerated immune response towards an antigen. Hypersensitivity is the most common manifestation in response to environmental xenobiotics. It can be caused by inhalation, ingestion or contact with a stimulant (Janeway et al., 2001). There are four types of hypersensitivities. Type I hypersensitivities are immediate hypersensitivities in response to allergens and are regulated by immunoglobulin E (IgE). These responses can be systemic (systemic anaphylaxis) or localized to a specific site (asthma, rhinitis, dermatitis) (Janeway et al., 2001). Type II hypersensitivities – also referred to as cytotoxic hypersensitivities – are caused by the interaction of IgG and IgM with the allergen. The immunoglobulins bind to an individual's own Ags on the surface of cells and signal cell death by

activating the complement pathway. This is observed when the incorrect blood type is administered (Janeway et al., 2001). Type III hypersensitivities are caused by the antigen which forms complexes with antibodies that often avoid clearing by macrophages due to their small size. These complexes then enter into the smaller vessels in the body where they activate the classical pathway of the complement system, which causes inflammation in the tissue, ultimately causing damage to the tissue. These damaging effects include: glomerulonephritis, rheumatoid arthritis and systemic lupus erythematosus (Eggleton 2013). Type IV hypersensitivities is also known as cell-mediated or delayed hypersensitivities. It is so named due to its presentation occurring at least 24-48 hours after exposure to an intracellular pathogen. Unlike the other hypersensitivity reactions, type IV hypersensitivity reactions do not rely on Abs to elicit a response. It is caused by the overstimulation of thymus (T) lymphocytes and macrophages which promotes the release of several cytokines, causing inflammation, and cell death (Warrington et al., 2011).

Autoimmunity refers to a condition where the immune system mounts an immune response to the body's own antigens (Ags). In a healthy immune system, the body has self-tolerance, where the immune system only reacts to foreign Ags and not host Ags (Janeway et al., 2001). During autoimmune responses the self-tolerance is lost, and autoantibodies can either target only one organ or it may attack the entire body, which can be seen in diabetes mellitus and lupus, respectively (De Jong and Van Loveren 2007).

Each of the four manifestations of immunotoxicity renders the functioning of the immune system obsolete and could result in severe damage to the body, by rendering the protective function of immune system inadequate (Konig 2011). It is thus necessary to identify various chemicals which have the potential to be xenobiotics and to determine their potential immunotoxic effects (Donner et al., 2010, Konig 2011)

Although several xenobiotics exist, one of the most progressive new material development fields producing potential xenobiotics is nanotechnology (Dobrovolskaia et al., 2009). As previously mentioned, the small size of nanoparticles (NPs) has allowed it to be used in several different industries (Abhilash 2010). With the increased interest in nanotechnology to improve applications in various industries, there is increased risk of exposure to nanoparticles in the environment. This also increases the exposure of NPs to the body (Dobrovolskaia et al., 2009).

Nanotechnology is a broad field which encompasses many different nanoparticles. It is therefore impossible to cover all nanoparticles and all their interactions in various environments in one study. Thus, for purpose of this research project, the focus will be on carbon quantum dots (CQDs). As a result of CQDs being employed in so many applications, particularly bioimaging, exposure to the body's internal environment is inevitable. CQDs will be in direct contact with immune cells if injected intravenously, the CQDs can thus modulate the functioning of these immune cells, therefore more work should be done to determine the immunomodulatory potential of these NPs so that they can be used safely.

### **3.4. Carbon Quantum Dots (CQDs)**

Carbon quantum dots (CQDs) are small, spherical carbon-based nanoparticles which have a size range between 1-10nm (Wang and Hu 2014). These carbon nanoparticles were accidentally discovered during the separation and purification of single-walled carbon nanotubes (SWCNTs) (Xu et al., 2004). During the synthesis of SWCNTs in 2004 by Xu and associates, they found that among the SWCNTs were highly fluorescent particles, which are now known as CQDs. Many other terms exist for CQDs, such as C-dots, carbon nanoparticles, quantum sized carbon dots and carbon nanodots (Kelarakis 2014).

Owing to their properties such as fluorescence, high solubility, high resistance to photobleaching, biocompatibility and low toxicity, CQDs have been studied extensively for their potential in biomedicine, optronics, sensors and catalysis (Shen et al., 2013, Wang and Hu 2014). Recently, CQDs have been studied extensively to replace semi-conductor quantum dots (QDs) such as CdSe and other heavy metals for bioimaging applications because they are less toxic and exhibit similar luminescence to semi-conductor QDs (Cao et al., 2007, Havrdova et al., 2016, Wang and Hu 2014, Wang et al., 2011a).

Following its discovery, several methods involving both top-down and bottom-up approaches have been employed to synthesize CQDs (Bayati et al., 2017, Wang and Hu 2014, Zhang and Yu 2015). During top-down methods, large carbon sources are cut down using concentrated oxidizing acids such as  $\text{HNO}_3$   $\text{H}_2\text{SO}_4$ /  $\text{HNO}_3$  mixture. Top-down synthesis is often considered as an expensive procedure because it requires costly apparatus (Esteves da Silva and Gonçalves 2011, Wang and Hu 2014). Bottom-up methods involve building up nanostructures via thermal carbonization and acid dehydration of suitable precursors (Liu et al., 2012, Kellarakis 2014). Via the bottom-up route, CQDs can be synthesized cheaply from virtually any precursor material containing carbohydrates, such as: grass, gelatine, orange and strawberry juice, bovine albumin and glycerol (Kellarakis 2014, Peng and Travas-Sejdic 2009, Wang et al., 2011a).

Several methods exist for CQDs synthesis utilizing diverse approaches and starting materials, with each combination producing NPs with variable properties (Wang and Hu 2014). In a study by Peng and Travas-Sejdic (2009) it was established that synthetic processes couldn't be altered in terms of time and starting material to produce CQDs with specific properties for their desired applications.

One drawback of some synthetic routes for CQDs to be employed in imaging is that CQDs produced, do not exhibit photoluminescence following synthesis (Kelarakis 2014). This was observed following CQDs synthesis via laser ablation (Sun et al., 2006). It was then established that the CQDs only displayed photoluminescence following passivation with poly- (ethylene glycol) (PEG) and it was thus concluded that passivation was a requirement for photoluminescence. The passivation agent, PEG is often used for CQDs because not only do they promote photoluminescence, but they are also neutral, and it does not reduce cell viability at 100µg/ml, which is the highest concentration required for bioimaging applications (Havrdova et al., 2016). CQDs possess several surface reactive groups, allowing for effective surface modifications such as passivation (Zhu et al., 2015).

Apart from passivation, the surface CQDs can also be modified through the functionalization of various compounds which alters the properties of the CQDs and ultimately determines the applications of the CQDs (Wang and Hu 2014). The ability of CQDs to bind to many different groups lies in its oxygen rich surface groups which allows for covalent bonding (Dimos 2016, Havrdova et al., 2016, Wang and Hu 2014). It is due to their biocompatibility and high surface functionalization potential that CQDs functions can be fine-tuned for specific functions in biomedicine, optoelectronics, catalysis and chemical sensors (Bayati et al., 2017). Wang et al (2011b), proposed a cheap synthetic route for photoluminescent CQDs without surface passivation. They synthesized CQDs via microwave irradiation using only glycerol and a phosphate solution. The CQDs were photoluminescent and they were shown to readily enter into *E.coli* and 293T cells. Wang et al (2011a) concluded that the synthesized CQDs were suitable for applications in biolabeling and bioimaging and that passivation was not necessary for CQDs to be photoluminescent as previously postulated.

Although several studies have reported that CQDs induce negligible cytotoxicity at concentrations sufficient for labelling (10-100 µg/ml), some CQDs have been shown to be cytotoxic. Many studies have concluded that the cytotoxicity caused by CQDs is as a result of the functional groups attached to the surface of the CQDs and not the CQDs itself (Havrdova et al., 2016, Yuan et al., 2017). Thus, according to Havrdova et al (2016), functional groups which are known to induce cytotoxicity should be used cautiously for clinical purposes.

On the other hand, very little work has been done to evaluate the immunological responses to CQDs. A study by Gao et al (2013) concluded that the injection of high doses of CQDs increased the production of type 1 thymus helper lymphocyte (Th1) and cytotoxic thymus lymphocytes (Tc), however these effects were not sufficient to induce morphological changes of the immune organs assessed. Thus, the mechanism by which CQDs modulate the immune system remains unclear. Gao and associates (2013) concluded that more systematic and profound studies are needed, and the pertinent testing guidelines for immunological evaluation of nanoparticles need to be formulated quickly.

As a result of the increased usage of CQDs (Bayati et al., 2017, Wang et al., 2013), human, animal and plant exposure to these NPs is inevitable and more studies are needed to determine the immunological responses to CQDs. The effects on CQDs on the immune system are important factors to consider as the immune cells are one the first groups of cells that CQDs may encounter in the bloodstream, (Kononenko et al., 2015). It has been reported by several studies that carbon nanotubes (CNTs) can induce allergic airway inflammation, pulmonary inflammation and inflammatory cytokines, interleukin 1 $\beta$  (IL-1 $\beta$ ), interleukin 6 (IL-6) and tumor necrosis factor alpha (TNF $\alpha$ ) under *in vitro* conditions. Due to CQDs being discovered as a by-product during synthesis of CNTs, it is a concern that CQDs may also cause immunological effects similar to

CNTs (Zhang et al., 2012). Therefore, it is of vital importance to determine the immunomodulatory effects of CQDs, as the immune system is responsible for the maintaining homeostasis and if its functioning is altered, it may result in illnesses (Kononenko et al., 2015).

The aim of the current study is to evaluate the effects of CDs on the murine macrophage cell line, RAW 264.7. In this work, murine macrophage RAW264.7 cells were used to explore different immunological responses of CQDs synthesized via microwave irradiation. Macrophages are commonly employed in primary toxicity studies as they offer a highly efficient defence system that can filter and remove particulate matter. Macrophages are also potent producers of immune mediators including cytokines and chemokines, which participate in antigen presentation. Owing to their importance in the immune system, various studies have investigated the effects of nanoparticles on macrophages both in cell culture system and *in vivo* (Barnett and Brundage 2010, Zhang et al., 2012). *In vitro* studies are preferred as they are both rapid, cost effective. In the present study, various parameters such as cell viability, inflammatory biomarkers, cytokines, chemokines and a proteome profile analysis were assessed. Carbon quantum dots have been shown to induce negligible toxicity, however when toxicity was observed, it was dependent in the surface coatings of the nanoparticles (Bayati et al., 2017, Dimos 2016, Havrdova et al., 2016, Wang et al., 2013). Only one study by (Gao et al., 2013) has assessed the immunomodulatory effects of CQDs and found that CQDs stimulates the immune system but does not cause any adverse effects.

### **3.5. Aim of this study**

- To utilize mammalian macrophage cell cultures to monitor the effects of carbon quantum dots on the immune system, using *in vitro* techniques.

- To identify molecular biomarkers that can be used in rapid bioassays to monitor adverse effects of heavy metals and nanoparticles.

### **3.6. Hypothesis**

H<sub>0</sub>: Carbon quantum dots have no immunomodulatory effects on RAW 246.7 macrophages.

H<sub>1</sub>: Carbon quantum dots have an immunomodulatory effect on RAW 246.7 macrophage.



## Chapter 4:

### Methods

#### 4.1. Nanoparticle Synthesis

The carbon quantum dots (CQDs) evaluated in this study were donated by the University of Missouri. The CQDs were both synthesized and characterized as published by Bayati et al (2017). In summary, CQDs were prepared by mixing glycerol (70% (v/v)) with 7.1 mM phosphate solution (pH 7.4) in a domestic oven (750 W) for 14 minutes. Transmission electron microscopy (TEM) (JEOL 1400, Peabody, MA, USA), revealed an average size range of 1–3 nm (Figure 4.1) and an average zeta potential of  $-16.83 \pm 1.40$  mV at a neutral pH in 1 mM sodium chloride (NaCl) (Figure 4.2)

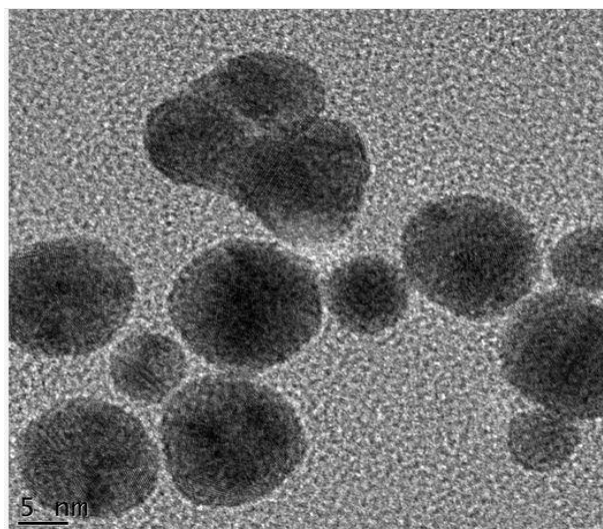


**Figure 4.1.** Visualization of carbon quantum dots via transmission electron microscopy (TEM).

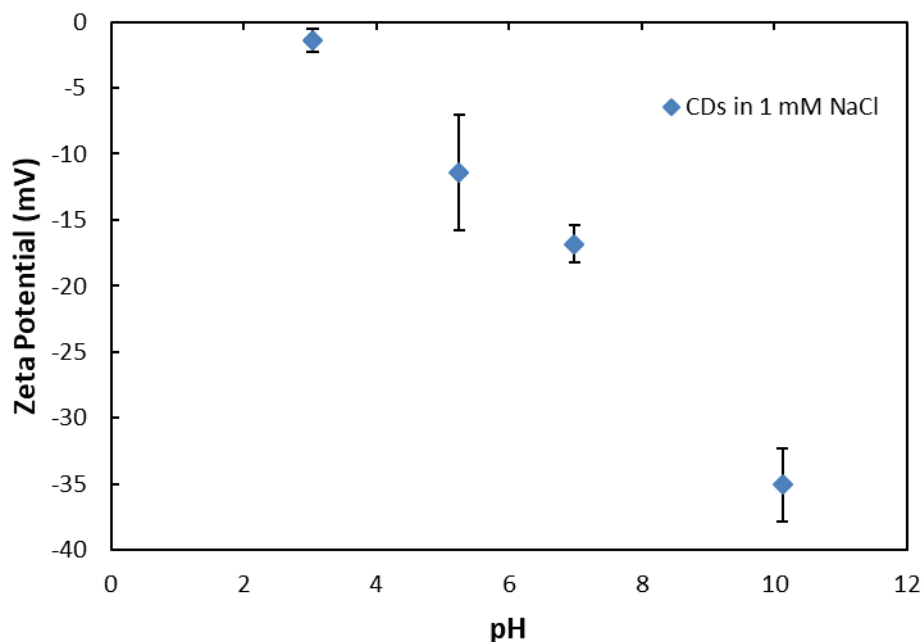


**Figure 4.2.** Zeta potential of carbon quantum dots under varying pH levels, while maintaining a constant ion concentration of 10 mM NaCl.

#### 4.2. Nanoparticle Preparation

Prior to cell exposure CQDs were freshly suspended to produce a stock of 10mg/ml in distilled water (dH<sub>2</sub>O). The nanoparticle mixture was then sonicated (Qsonica, LLC. Misonix sonicators, XL-200 Series, Connecticut, USA) in 20 second bursts on ice for a total of 5 minutes

#### 4.3. Cell Culture Reagents

Cell culture was performed aseptically. RAW 264.7 cells, derived from murine macrophages, were obtained from American Type Culture Collection (ATCC TIB-71, Manassas, VA, USA). RAW 264.7 cells were grown in 75cm<sup>2</sup> tissue culture flasks (Sigma-Aldrich, St. Louis, Missouri, United States). Culture media always contained, Dulbecco's Modified Eagle's Medium (DMEM) (Lonza, Basel, Switzerland), 1% v/v antibiotic/anti-mycotic (penicillin/streptomycin) (Sigma-Aldrich), 0.5% v/v gentamycin (Sigma-Aldrich) and 1% v/v glutamax (Sigma-Aldrich). Complete media

comprised of culture media supplemented with 10% v/v heated-inactivated fetal-bovine serum (FBS) (Thermo Fisher Scientific, Waltham, Massachusetts, United States). Nanoparticle-stimulated media contained culture media and CQDs of various concentrations. Lipopolysaccharide-stimulated media consisted of culture media in the presence of 1 µg/ml lipopolysaccharide (LPS) (Sigma-Aldrich). Cells were maintained at 37°C in a humidified incubator of 5% CO<sub>2</sub> (NUAIRE™, Doncaster, United Kingdom). Cells were sub-cultured every 2-3 days once they've reached 80-90% confluence.

#### **4.4. Cells Exposure to CQDs**

When cells were 80-90% confluent, cells were re-suspended in 10% complete medium to give 10<sup>5</sup> cells/ml. RAW 264.7 cells were seeded at 400 µl/well in 24 well microtiter culture plates (Nunc, Denmark). The cells were incubated at 37°C with 5% CO<sub>2</sub> until 80-90% confluent (72 hours). The media was then removed from the wells and 400µl of culture media, supplemented with 2.5% FBS was added. This was followed by the addition of 400µl of nanoparticle-stimulated media, resulting in final CQD concentrations between 0-500 µg/ml. The positive and negative control only received 400µl of culture media. After two hours, 200µl of LPS-stimulated culture media was added to the positive control and 200 µl of culture media was added to the negative control and to the wells containing CQD-stimulated media. The cells were then incubated overnight (18 hours) at 37°C with 5% CO<sub>2</sub>. Samples were assayed in triplicate.

Following incubation, the supernatants were removed and centrifuged for 5 min at 12100 rcf (Super mini centrifuge, miniStar Plus, China). Thereafter supernatants were assayed for Nitric Oxide (NO), Interleukin 6 (IL-6), Macrophage inflammatory protein-1 alpha (MIP 1α), Macrophage inflammatory protein-1 beta (MIP 1β), Macrophage inflammatory protein-2 (MIP 2) and proteome profiling.

#### **4.5. Cell Viability**

Cell viability was determined using the stable water tetrazolium salt, WST-1 (Roche, Basel, Switzerland). During this assay the WST-1 reagent is converted to a formazan dye by cellular mitochondrial dehydrogenases, this conversion can only be performed by live cells. Thus, the amount of formazan formed is directly proportional to the number of viable cells present (Cell Viability Assays - Assay Guidance Manual - NCBI Bookshelf).

After the incubation with various additives, cell culture supernatants were removed, and the wells were washed with Dulbeccos Phosphate Buffered Saline (DPBS) (Lonza). Two hundred microliters of WST-1 reagent (1:10 in culture media) was added to each well. Following a 60-minute incubation at 37°C in 5% CO<sub>2</sub>, 50µl of WST-1 reagent was removed from each well and transferred to a 96 well plate (Greiner bio-one, Kremsmünster, Austria) before being read at 450nm (Multiskan Ex, Thermo Fisher Scientific, Waltham, Massachusetts, United States).

#### **4.6. Nitric Oxide (NO)**

The Greiss reaction was used to determine the amount of nitrite in the samples. During the Greiss reaction, nitrate is converted to nitrite by the enzyme nitrate reductase. The amount of nitrite present is an indicator of the amount of NO in the sample (Bryan and Grisham 2007). Following cell culture exposure to various conditions, supernatants were transferred to a 96 well flat bottom plate (Greiner bio-one) at room temperature. Each well received 50µl of the respective supernatant. Nitrite standards were included on each plate. The range of the standard was between 1.562-100µM. Greiss reagent was prepared by 1:1 solution of 1% Sulfanilamide (Sigma-Aldrich) and 0.1% N-1-naphthylethylenediamine dihydrochloride (Sigma-Aldrich) in 2.5% phosphoric acid. Following preparation, 50µl of Greiss reagent was added to each well containing either the nitrite

standards or culture supernatant. The plate was then incubated at 37°C for 15 minutes, thereafter, the absorbance was read at 540nm (Multiskan Ex, Thermo Electron Corporation).

#### **4.7. Interleukin 6 (IL-6)**

The mouse IL-6 cytokine ELISA kit (eBioscience, Ready-Set-Go, Thermo Fisher Scientific) was used for the precise measurement of mouse macrophage IL-6 levels. The assay was performed according to manufacturer's instructions in a 96 well maxisorb plate (Nunc). The plate was coated with capture antibody overnight at 4°C. Serial dilutions of murine IL-6 standard was prepared and added to the plate at a range of 0 to 2000pg/ml. Lipopolysaccharide-stimulated cell culture supernatants were diluted (1/40) while LPS-unstimulated cell culture supernatants were diluted (1/5) in assay diluent and pipetted in to their respective wells. After two hours, the wells were washed and detection antibody, specific for IL-6 was added to the wells. Following a 1-hour incubation, wells were thoroughly washed to remove all unbound reactants and ultrasensitive chromogenic 3,3',5,5'-Tetramethylbenzidine (TMB) (Sigma-Aldrich) membrane substrate was added to the plate for 15 minutes before the reaction was stopped by adding 2M H<sub>2</sub>SO<sub>4</sub> to each well. The optical densities of the colour reaction were read at 450nm (Multiskan Ex, Thermo Electron Corporation). The amount of IL-6 produced by the cells was calculated from the standard curve of known amounts of murine IL-6.

#### **4.8. Murine MIPs (MIP-1 $\alpha$ , MIP-1 $\beta$ and MIP-2) ELISAs**

Mouse ELISA kits for MIP-1 $\alpha$ , MIP-1 $\beta$  and MIP-2 (R and D Systems, Minneapolis, MN, USA) were purchased for the quantification of the respective chemokines. The experiments were carried out according to manufacturer's instructions. All samples were diluted in assay diluent, 1% w/v human serum albumin (HSA, Western Province Blood Transfusion Services South Africa) in 1X phosphate buffered saline (PBS) (Lonza) was used as assay diluent. Nunc maxisorp plates were

used for the assays. Plates were coated with respective capture antibodies for each chemokine, murine MIP-1 $\alpha$ , MIP-1 $\beta$  and MIP-2, overnight at 4°C. Serial dilutions of standard amounts of murine MIP-1 $\alpha$ , MIP-1 $\beta$  and MIP-2 were prepared and added into the 96-well plates. For MIP-1 $\alpha$ , LPS-stimulated cell culture supernatants and LPS-unstimulated cell culture supernatants were diluted (1/2000) v/v and (1/270) v/v in assay diluent, respectively. For MIP-1 $\beta$ , LPS-stimulated cell culture supernatants and LPS-unstimulated cell culture supernatants were diluted (1/5000) v/v and (1/20) v/v in assay diluent, respectively. Lastly, MIP-2 levels were measured by diluting LPS-stimulated cell culture supernatants and LPS-unstimulated cell culture supernatants in assay diluent, (1/500) v/v and (1/20) v/v, respectively. Prepared supernatants were added to their respective wells in a 96 -well plate. After 2 hours the wells were washed and detection antibodies, specific for MIP1 $\alpha$ , MIP1 $\beta$  and MIP2 were added to the wells. After a 2 hour incubation, wells were thoroughly washed to remove all unbound reagents and TMB membrane substrate was added to the plate for 5 minutes before the reaction was stopped by adding 2M H<sub>2</sub>SO<sub>4</sub> to each well. The optical densities of the colour reaction were read at 450nm (Multiskan Ex, Thermo Electron Corporation). The amount of MIP-1 $\alpha$ , MIP-1 $\beta$  and MIP-2 produced by the cells was calculated for the standard curve of known amounts of murine MIP-1 $\alpha$ , MIP-1 $\beta$  and MIP-2.

#### **4.9. Murine Cytokine Proteome Profiling Array**

The Proteome Profiler antibody array (R and D systems, Bio-Techne, Minneapolis, Minnesota, United States) was used to simultaneously quantify the cytokines and chemokines present in RAW 264.7 cell supernatants exposed to LPS, CQDs and under basal conditions. The nitrocellulose membrane used in this assay, was pre-coated in duplicate, with 40 capturing antibodies for various cytokines. The kit contained all the reagents for the assay and was performed according to the manufacturer's instructions. Pre-coated membranes were blocked with assay blocking buffer. Five

hundred microliters of cell culture supernatants from the negative control, positive control and 500µg/ml CQD-stimulated samples were mixed with buffers and detection antibody. The sample and detection cocktail was then added to each respective membrane for overnight incubation on a rocking platform at 4°C. Membranes were washed and protein was detected through the addition of TMB membrane substrate (Thermo Fisher Scientific) to reveal sample-antibody complexes labelled with streptavidin-HRP. Chromogenic 3,3',5,5'-Tetramethylbenzidine membrane substrate (Thermo Fisher Scientific) was used instead of the kit's chemiluminescent reagent mix for visualization and quantification of cytokines and chemokines because it provided clearer visuals. The reaction was stopped by removing the TMB substrate and adding dH<sub>2</sub>O onto the membranes. Photographs were taken after the dH<sub>2</sub>O on the membrane was dried.

#### **4.10. Quantification of Pixel Density for Cytokine Blot**

Membrane images were quantified using image processing and analysis ImageJ (version 1.4.3.67, National Institutes of Health). Levels of cytokines and chemokines were expressed as a percentage of the reference spot. Microsoft Excel was used to calculate the percentage which is expressed as mean ± standard deviation (SD).

#### **4.11. Statistical Analysis**

All experiments were performed in triplicate and the data was calculated using Microsoft Excel. The data are presented as mean ± standard deviation (SD). Statistical analysis of differences was performed by SigmaPlot Version 12.0 (Systat software, Inc) using one-way analysis of variance (ANOVA). The P-value < 0.001 was considered as statistically significant.

## Chapter 5:

### Results

#### 5.1. The Effects of CQDs on RAW 264.7 Cell Viability

RAW cell viability, under basal conditions was significantly reduced ( $P < 0.001$ ) by CQD concentrations, 62.5 and 250  $\mu\text{g/ml}$  compared to the 0  $\mu\text{g/ml}$  CQD control (Figure 5.1). The other CQD concentrations evaluated in this study caused no effect on viability compared to the 0  $\mu\text{g/ml}$  CQD control.

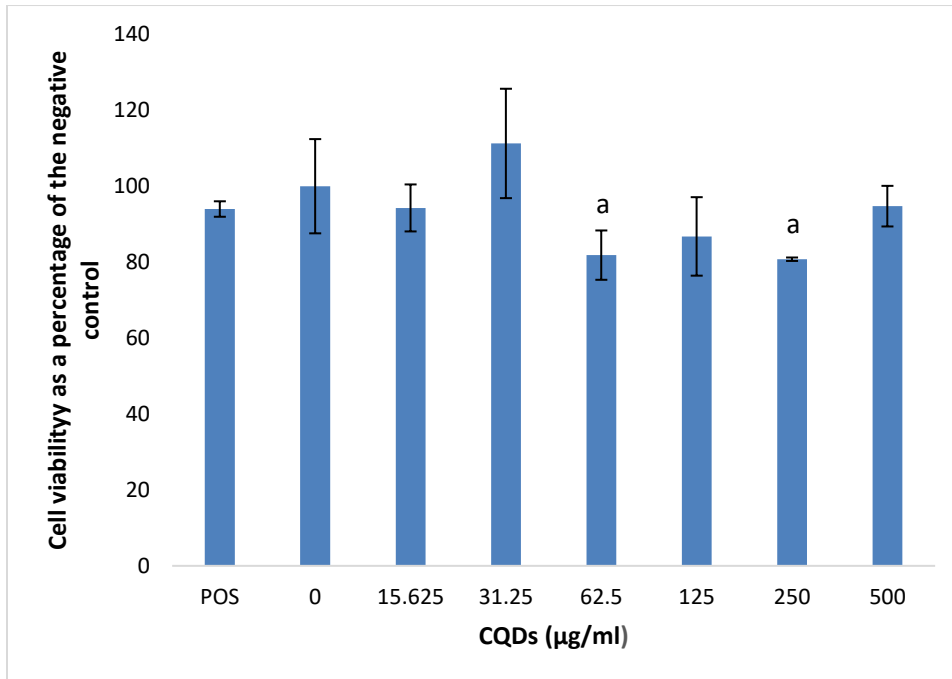


**Figure 5.1.** Cell viability of RAW 264.7 cells exposed to CQDs. The results are presented as mean  $\pm$  SD with  $n = 9$ . Significance demarcated by: a- significantly different ( $P < 0.001$ ) compared to 0  $\mu\text{g/ml}$  CQD control.



## 5.2. The Effects of CQDs on the Inflammatory Biomarker NO Secretion by RAW 264.7 Cells

At the tested concentrations, CQDs had no effects on NO production compared to the 0  $\mu\text{g/ml}$  CQD control (Figure 5.2). RAW cells treated with LPS in the absence of CQDs was included as a positive control for inflammation, and produced significantly higher NO than the 0 $\mu\text{g/mL}$  CQDs control ( $P < 0.001$ ).

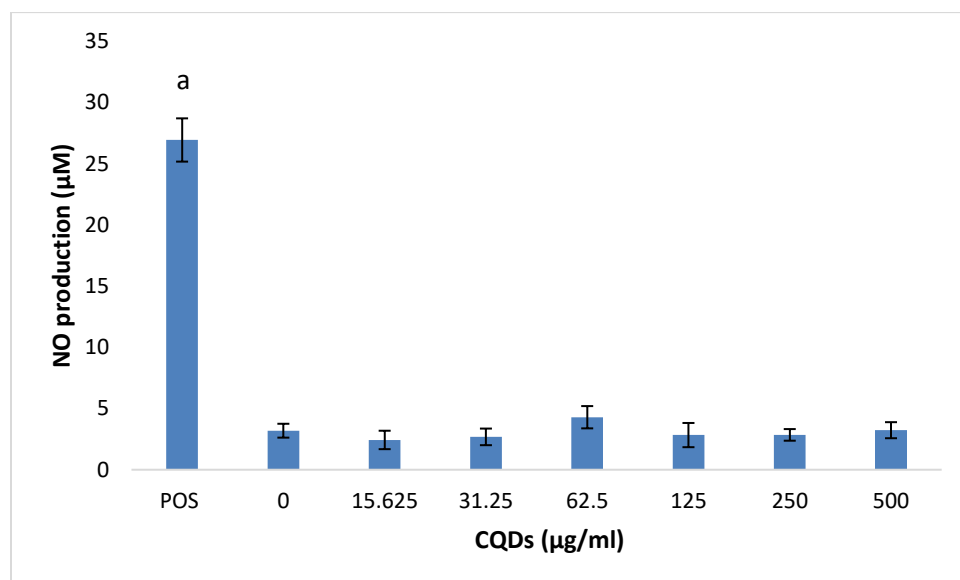


**Figure 5.2.** NO levels of RAW 264.7 cell cultures exposed to CQDs. The results are presented as mean  $\pm$  SD with  $n = 9$ . Significance demarcated by: a- significantly different ( $P < 0.001$ ) compared to the 0  $\mu\text{g/ml}$  CQD control.

## 5.3. The Effects of CQDs on the Inflammatory Biomarker IL-6 Secretion Using RAW 264.7 Cells

CQD concentrations  $\leq 31.25$   $\mu\text{g/ml}$  had no effect on IL-6 in an unstimulated environment (Figure 5.3). However, CQD concentrations  $\geq 62.5$   $\mu\text{g/ml}$  significantly ( $P < 0.001$ ) inhibited IL-6 synthesis from cells under basal conditions compared to the 0  $\mu\text{g/ml}$  CQD control. The positive control ( $56748 \pm 9591.8$  pg/ml IL-6) is not included in the figure.

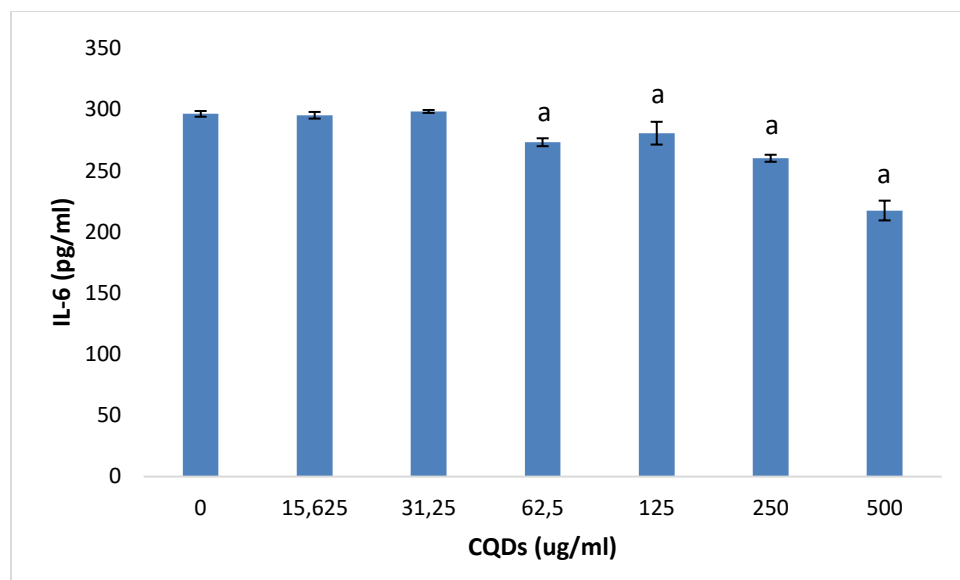


**Figure 5.3.** IL-6 levels of unstimulated RAW 264.7 cell cultures exposed to CQDs. The results are presented as mean  $\pm$  SD with  $n = 9$ . Positive control (+ LPS) not presented ( $56\,748 \pm 9\,591.8$  pg/ml IL-6). Significance demarcated by: a- significantly different ( $P < 0.001$ ) compared to  $0$   $\mu\text{g/ml}$  CQD control.

#### 5.4. The Effects of CQDs on Chemokines Secretion Using RAW 264.7 Cells

##### 5.4.1. The Effects of CQDs on MIP-1 $\alpha$ Secretion Using RAW 264.7 Cells

CQD concentrations  $\leq 31.25$   $\mu\text{g/ml}$  did not affect MIP-1 $\alpha$  synthesis from RAW cells under unstimulated conditions (Figure 5.4). However, CQD concentrations  $\geq 62.5$   $\mu\text{g/ml}$  significantly up regulated ( $P < 0.002$ ) MIP-1 $\alpha$  synthesis under basal conditions compared to the negative control. The positive control (LPS only) is not presented ( $1\,637\,093 \pm 199\,883.8$  pg/ml MIP-1 $\alpha$ ).

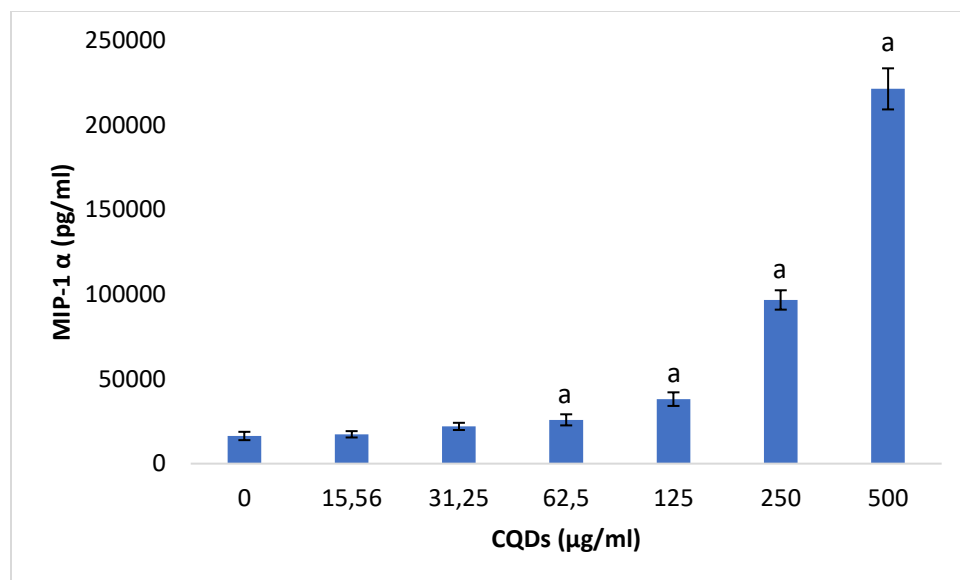


**Figure 5.4.** MIP-1 $\alpha$  levels of unstimulated RAW 264.7 cell cultures exposed to CQDs. The results are presented as mean  $\pm$  SD with n = 9. Positive control (+ LPS) not presented (1 637 093  $\pm$  199 883.8 pg/ml MIP-1 $\alpha$ ). Significance demarcated by: a- significantly different (P < 0.002) compared to 0  $\mu$ g/ml CQD control.

#### 5.4.2. The Effects of CQDs on MIP-1 $\beta$ Secretion Using RAW 264.7 Cells

MIP-1 $\beta$  synthesis was not affected by CQD concentrations  $\leq$  125  $\mu$ g/ml (Figure 7.5). CQD concentrations  $\geq$  250  $\mu$ g/ml significantly upregulated (P < 0.001) MIP-1 $\beta$  synthesis from RAW cells under basal conditions compared to the negative control. The positive control, LPS (343 965  $\pm$  52 044 pg/ml MIP-1 $\beta$ ) is not presented on figure 5.5.

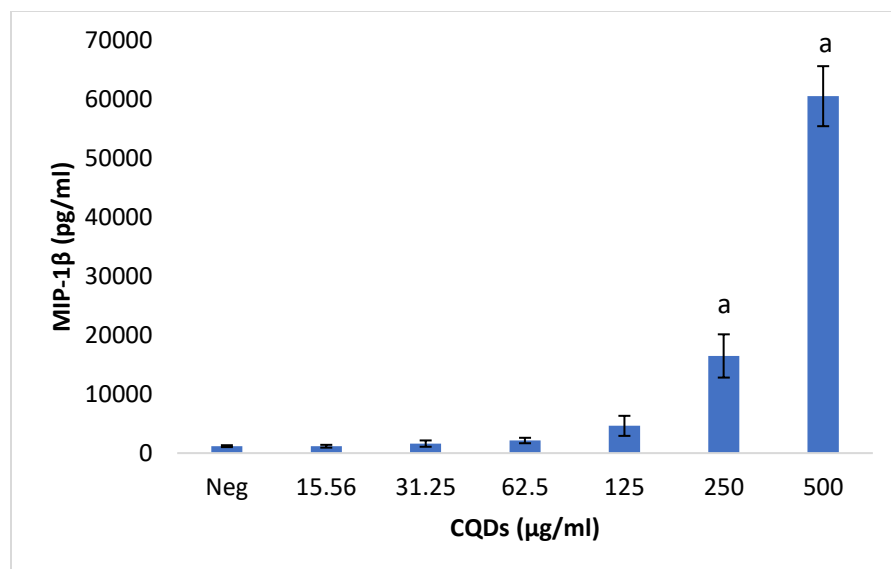


**Figure 5.5.** MIP-1 $\beta$  levels of unstimulated RAW 264.7 cell cultures exposed to CQDs. The results are presented as mean  $\pm$  SD with  $n = 9$ . Positive control (+ LPS) not presented ( $343\,965 \pm 52\,044$  pg/ml MIP-1 $\beta$ ). Significance demarcated by: a- significantly different ( $P < 0.001$ ) compared to 0  $\mu$ g/ml CQD control.

#### 5.4.3. The Effects of CQDs on MIP-2 Secretion Using RAW 264.7 Cells

MIP-2 synthesis from RAW cells exposed to CQD concentrations mimicked the MIP-1 $\beta$  data under basal conditions (Figure 5.5). MIP-2 was unaffected by CQD concentrations  $\leq 125$   $\mu$ g/ml (Figure 5.6). However, CQD concentrations  $\geq 250$   $\mu$ g/ml significantly upregulated ( $P < 0.001$ ) MIP-2 synthesis from RAW cells under unstimulated conditions. The LPS stimulated positive control ( $302\,089 \pm 68\,868$  pg/ml MIP-2) is not presented on figure 5.6.

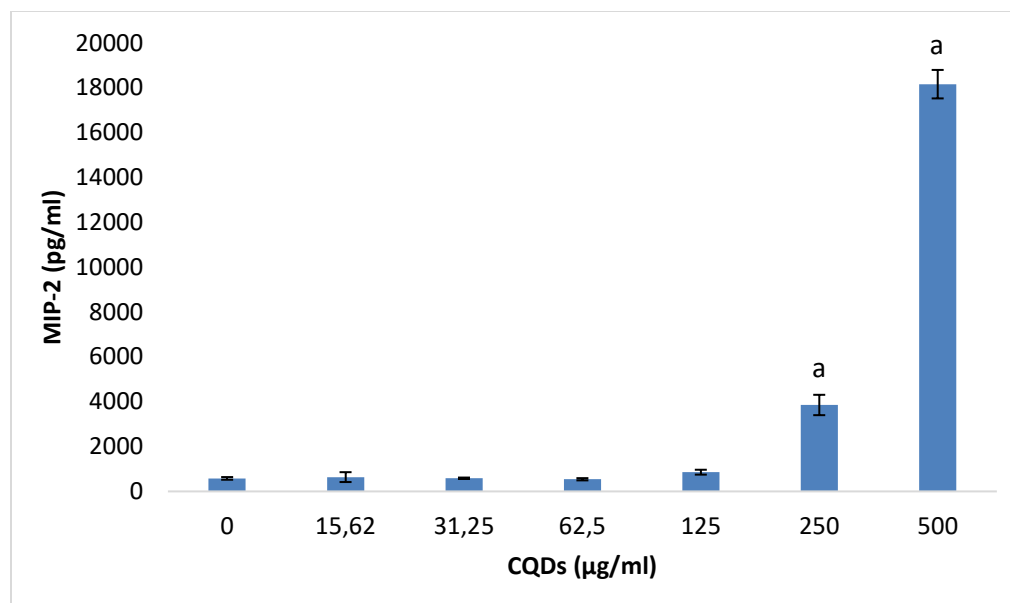


**Figure 5.6.** MIP-2 levels of unstimulated RAW 264.7 cell cultures exposed to CQDs. The results are presented as mean  $\pm$  SD with  $n = 9$ . Positive control (+ LPS) not presented ( $302\ 089 \pm 68\ 868$  pg/ml MIP-2). Significance demarcated by: a- significantly different ( $P < 0.001$ ) compared to 0  $\mu\text{g/ml}$  CQD control.

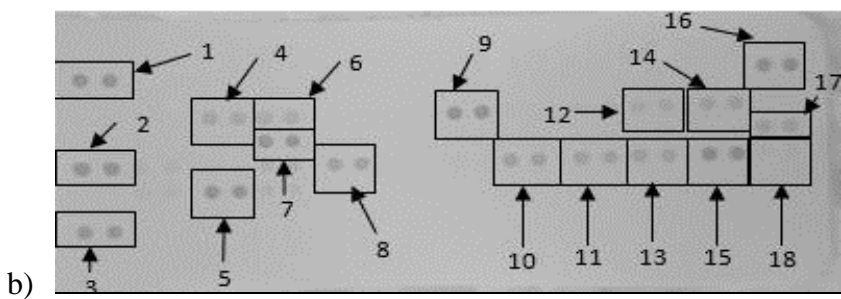
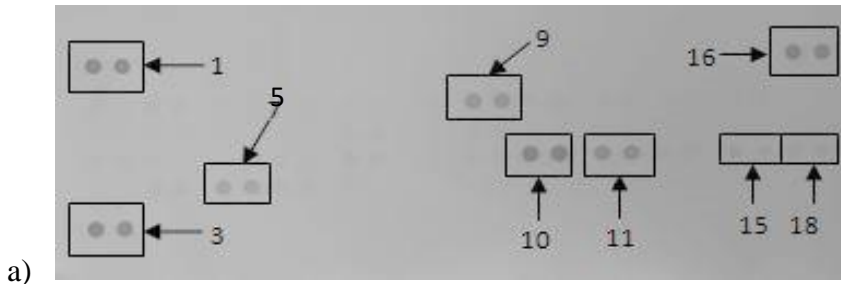
### 5.5. The Effects of CQDs on the Secretory Cytokine and Chemokine Profile of RAW 264.7 Cells

Membranes assayed with culture supernatants of RAW 264.7 cells exposed to culture media only, LPS-stimulated media, and cells exposed to media containing 500  $\mu\text{g/ml}$  CQDs in the absence of LPS allowed for the simultaneous detection of an array of cytokines and chemokines (Figure 5.7). Visual inspection of the membranes showed that RAW cells exposed to the positive control, allowed the cells to synthesize certain proteins that were not synthesized by cells exposed to only culture media 0  $\mu\text{g/ml}$  CQDs only (Table 5.1.). The proteins secreted by LPS-stimulated media and not by culture media include, IFN $\gamma$ -inducible protein-10 (IP-10), Granulocyte-colony stimulating factor (G-CSF), Granulocyte-macrophage colony-stimulating factor (GM-CSF), IL-6,

MIP-2, Monocyte chemoattractant protein 1 (MCP-1)/JE, Interleukin 1 receptor agonist (IL-1ra), Interleukin 27 (IL-27) and Interleukin 1  $\beta$  (IL- $\beta$ ).

On the other hand, certain proteins were significantly ( $P \leq 0.001$ ) upregulated by cells exposed to 500  $\mu\text{g/ml}$  CQDs compared to the 0  $\mu\text{g/ml}$  CQD control. These proteins include  $\text{TNF}\alpha$ , IP-10, G-CSF, GM-CSF, JE, MIP-1 $\alpha$ , MIP-1 $\beta$ , MIP-2 and IL-1ra.

The CQDs seem to be inflammatory from the nature of the cytokines they induce. However, the CQDs do not produce all the cytokines produced by the positive inflammation stimulant (LPS), these include, IL-6, IL-1 $\beta$ , IL-27 and Stromal cell-derived factor 1 (SDF-1).



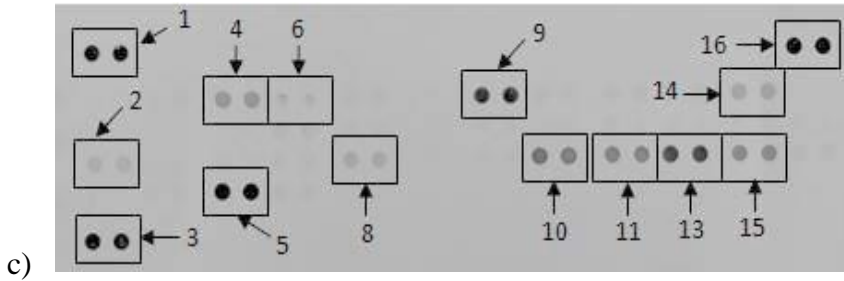


**Figure 5.7.** The effect of CQDs on RAW 264.7 cells. Cells were incubated with (a) culture media only (negative control), (b) LPS-stimulated media (positive control) and (c) 500 µg/ml CQDs in the absence of LPS. Supernatants were assayed using the proteome profiler array as described in the methods section. Cytokines/chemokines that were detected were allocated numbers: 1, 3, and 16 are reference spots, 2- IP-10; 4- G-CSF; 5- TNF- $\alpha$ ; 6- GM-CSF; 7- IL-6; 8- JE; 9-sICAM-1; 10- MIP-1 $\alpha$ ; 11- MIP-1 $\beta$ ; 12- IL-1 $\beta$ ; 13- MIP-2; 14- IL-1ra; 15- RANTES; 17- IL-27; 18-SDF-1.

**Table 5.1.** The effects of CQDs on RAW 264.7 cells expression of chemokines and cytokines. Cells not stimulated with LPS after treatment with medium only (negative control), medium containing LPS (positive control) or medium containing 500 µg/ml CQDs. Membranes were subjected to chromogenic exposure. ‘Yes’ represents the presence while ‘No’ represents the absence of cytokines and chemokines in response to the exposures, to the naked eye.

<b>Cytokines and Chemokines</b>	<b>Location</b>	<b>Positive Control</b>	<b>Negative Control</b>	<b>500µg/ml</b>
Reference Spots	1, 3, 16	Yes	Yes	Yes
IP-10	2	Yes	No	Yes
G-CSF	4	Yes	No	Yes
TNF- $\alpha$	5	Yes	Yes	Yes
GM-CSF	6	Yes	No	Yes
IL-6	7	Yes	No	No
JE	8	Yes	No	Yes
sICAM	9	Yes	Yes	Yes
MIP-1 $\alpha$	10	Yes	Yes	Yes
MIP-1 $\beta$	11	Yes	Yes	Yes
IL-1 $\beta$	12	Yes	No	No
MIP-2	13	Yes	No	Yes
IL-1ra	14	Yes	No	Yes
RANTES	15	Yes	Yes	Yes
IL-27	17	Yes	No	No
SDF-1	18	Yes	Yes	No



## **Chapter 6:**

### **Discussion**

Carbon quantum dots (CQDs) are relatively new nanoparticles (NPs) that have been shown to exhibit high levels of photoluminescence, hydrophilicity, low toxicity, robust chemical inertness, high resistance to photo-bleaching and high biocompatibility compared to heavy metal quantum dots (Bayati et al., 2017, Wang et al., 2011b). Due its properties, CQDs have been researched to be used in various biomedical applications such as imaging, drug delivery and detection (Gao et al., 2013, Havrdova et al., 2016, Peng et al., 2017).

As previously mentioned, CQDs have been increasingly researched to replace heavy metal semiconductor quantum dots. However, CQDs must be fluorescent, cheaper to produce and non-toxic to effectively replace heavy metal semiconductor quantum dots (Wang et al., 2011b). Many groups have thus utilized an array of methodologies and materials to synthesize CQDs and evaluated them for specific applications. The increased production of CQDs leads to increased potential for human and environmental exposure. Although CQD production has increased, the same cannot be said for research regarding the safety associated with exposure to CQDs.

Therefore, the objective of this study was to reduce the lack of information regarding CQDs by evaluating the cytotoxic and immunomodulatory potential of CQDs on RAW 264.7 macrophages. Studies have evaluated the effects of CQDs on cell viability/cytotoxicity (Havrdova et al., 2016, Sun and Lei 2017, Tao et al., 2017, Wang et al., 2011b, Yang et al., 2009). However, through a google scholar search for, ‘Carbon quantum dots and the immune system’, only one study by (Gao et al., 2013) has evaluated the effects of CQDs on the immune system.

In the present study, macrophages were chosen as an *in vitro* model because these immune cells will be the first to be exposed to CQDs following systemic exposure in humans (Bertrand and Leroux 2012, Dobrovolskaia et al., 2009, Dobrovolskaia and McNeil 2007).

Exposing RAW cells to varying concentrations of CQDs showed that 62.5µg/ml and 250µg/ml CQDs, significantly ( $P < 0.001$ ) reduced cell viability compared to the 0µg/ml CQD. All other concentrations of CQDs exhibited no significant ( $P > 0.010$ ) effects on the viability of the RAW cells compared to the 0µg/ml. This supports previous data on CQDs exhibiting low toxicity (Shen et al., 2013, Wang and Hu 2014).

Low levels of CQD-induced cytotoxicity was also seen in a study by Kang et al (2015) who evaluated the *in vitro* cytotoxic effects of free carbon dots (CDs) and carbon-nanodot-conjugated Fe-aminoclay (CD-FeAC) using 3 (4,5-dimethylthiazol-2-yl)-2,5 diphentyltetrazolium bromide (MTT) viability and neutral red (NR) assays. At 1000µg/ml, CD-FeAC caused approximately 20% loss in viability of Hela cells while no reduction in cell viability was observed in normal cells up to 1000µg/ml. At concentrations up to 1000µg/ml, free CDs caused no cytotoxicity, which is contradictory to the results in the present study where CQD concentrations below 1000µg/ml, at 62.5 and 250µg/ml caused significant ( $P < 0.001$ ) reduction in cell viability, which was not consistent with Kang et al (2015). This variation in activity could be due to the utilization of different synthetic methods and precursors as the mode of synthesis which could ultimately lead to the variation in CQDs reactivity (Arora et al., 2012, Elsaesser and Howard 2012, Oberdörster et al., 2005, Zoroddu et al., 2014).

Surface modification of CQDs may also result in CQDs having different reactivity as the surface of CQDs influences the way NPs interacts in its environment (Dobrovolskaia and Mc Neil 2007,

Wang et al., 2011b, Wang and Hu 2014). A study by Wang et al (2011b) investigated the cytotoxic effects of CQDs functionalized with O, O'-bis(3-aminopropyl) polyethylene glycol (PEG1500N) poly(propionylethyleneimine-co-ethyleneimine)(PPEI-EI), polyethyleneimine (PEI), polyallyl amine (PAA). They reported toxicity induced by CQDs was dependant on types of functional groups attached to the CQDs.

Exposure of CQDs to RAW cells at the tested concentrations resulted in no significant ( $P > 0.010$ ) changes on nitric oxide (NO) secretion compared to the  $0\mu\text{g/ml}$  CQD sample. Similar results were obtained for interleukin-6 (IL-6) secretion, where CQDs concentrations  $\leq 31.25\mu\text{g/ml}$  caused no significant ( $P > 0.010$ ) changes in IL-6 secretion when compared to the  $0\mu\text{g/ml}$ . A similar study by Gao et al (2013) found that the spleens of mice exposed to varying concentrations of CQDs did not cause any significant changes in the secretion of Interleukin-4 and 12 (IL-4 and IL-12), Interferon-gamma (INF-  $\gamma$ ) and Tumor necrosis factor- $\alpha$  (TNF- $\alpha$ ). However, unlike Goa et al 2013, in the present study CQD concentrations  $\geq 62.5\mu\text{g/ml}$  caused a significant ( $P < 0.001$ ) reduction in IL-6 secretion when compared to the  $0\mu\text{g/ml}$  CQDs sample. As an important acute phase cytokine, IL-6 functions by activating inflammatory cells during acute inflammatory response. Decreased levels of IL-6 in response to CQDs suggests that CQDs plays an immunosuppressive role under basal conditions and could lead to increased susceptibility to infection (Gruys et al., 2005). Low IL-6 secretion is further corroborated with absence of IL-6 from  $500\mu\text{g/ml}$  CQD sample in the proteome profiling. Lack of IL-6 and NO could be as a result of CQDs affecting these inflammatory genes.

CQDs caused no significant ( $P > 0.010$ ) effects on macrophage inflammatory protein one alpha (MIP-1 $\alpha$ ) levels at concentrations  $\leq 31.25\mu\text{g/ml}$  when compared to the  $0\mu\text{g/ml}$  CQDs sample.

However, exposure of RAW cells to CQD concentrations  $\geq 62.5\mu\text{g/ml}$  caused significant ( $P < 0.002$ ) dose dependant increase of MIP-1 $\alpha$  secretion when compared to the  $0\mu\text{g/ml}$  CQDs sample.

In response to CQDs, macrophage secretion of MIP-1 $\beta$  and MIP-2 responded in the same manner, where concentrations  $\leq 125\mu\text{g/ml}$  caused no significant ( $P > 0.010$ ) changes on MIP-1 $\beta$  and MIP-2 compared to the control. Concentrations  $\geq 250\mu\text{g/ml}$  significantly ( $P < 0.001$ ) increased the production of both, MIP-1 $\beta$  and MIP-2 compared to the  $0\mu\text{g/ml}$  control.

Taken together, the data generated from the MIP ELISAs and Proteome profiling assays proves that RAW cell exposure to CQDs induces the release of an array of pro-inflammatory markers, mostly markedly TNF $\alpha$ , MIPs, IP-10, G-CSF, GM-CSF, and JE. Tumor necrosis factor alpha is predominantly produced by macrophages and plays a vital role in regulating cytokine production (Parameswaran and Patial 2010). The macrophage inflammatory proteins MIP-1 $\alpha$ , MIP-1 $\beta$  and MIP-2 are known for their chemotactic properties for leukocytes in response to injury, infection and cancer (Driscoll 1994). Secreted in response to interferon-gamma, one of IP-10 prominent roles, is the chemo-attraction for monocytes/macrophages, T cells, natural killer (NK) cells, and dendritic cells (Dufour et al., 2002) One of G-CSF's major functions is to influence the maturation and release of neutrophils from the bone marrow and enhance their chemotactic and phagocytic functions. Unlike G-CSF, which specifically promotes neutrophil proliferation and maturation, GM-CSF affects more cell types, especially macrophages and eosinophils (Mehta et al., 2015, Shi et al., 2006) lastly JE recruits monocytes, memory T cells, and dendritic cells to the sites of inflammation produced by either tissue injury or infection (Luo et al., 1994). In addition to the secretion of pro-inflammatory molecules,  $500\mu\text{g/ml}$  CQDs also significantly ( $P < 0.001$ ) upregulated the secretion of the anti-inflammatory cytokine, Interleukin-1 Receptor Antagonist (IL-1ra). IL-1Ra is a naturally occurring inhibitor of IL-1. When IL-1Ra binds to the IL-1 receptor, it blocks the binding of IL-1 and thereby preventing pro-inflammatory signal from IL-1 receptor (Jylhä et al., 2007) Although the secretion of cytokines may not be detrimental, persistent increased production in response to CQDs, could lead to the

overstimulation of immune responses, which could further progress to chronic inflammation, ultimately leading to inflammatory diseases (Konig 2011).

## Chapter 7:

### Conclusion and Future Perspectives

#### 7.1. Conclusion

In the current study, the effects of non--functionalized carbon quantum dots (CQDs) on cell viability and inflammatory responses were assessed using RAW 264.7 cells. The CQDs reduced RAW 264.7 cell viability at concentrations above 62.5 $\mu$ g/ml.

Exposure of CQDs to RAW cells, caused no effects on the inflammatory molecules NO and caused a reduction in IL- 6 secretion at concentrations above 62.5 $\mu$ g/ml. However, proteome profiling analysis showed that exposure to 500 $\mu$ g/ml CQDs, stimulated the secretion of TNF- $\alpha$  by RAW cells. Based on data generated from ELISAs and proteome profiling assays, RAW cell exposure to CQDs promotes the secretion of chemokines. These chemokines include, TNF $\alpha$ , MIPs, IP-10, G-CSF, GM-CSF, and JE, which has the potential to be used a biomarkers for CQDs exposure. The mechanism of CQDs immunomodulatory effects is minimal, and more research is needed to further understand how and CQDs modulate the immune system.

#### 7.2. Future Perspectives

In the present study, RAW 264.7 cells exposure to CQDs was only 18 hours, producing data for acute exposure to CQDs. Longer exposures would provide data for the determination of the effects of chronic exposure CQDs. In addition to the assays used in the present, more cellular tests, such as ROS generation, membrane integrity and genotoxicity assays could be done to determine cell responses to CQDs, allowing for a more in-depth understanding of the mode of action of CQDs. The current study was an *in vitro* study which represents an isolated depiction of the potential effects of CQDs on the immune system. Although an *in vitro* model provides insights into the

potential effects, an *in vivo* model has the potential to provide a better understanding of the mechanism of how CQDs may affect the entire immune system and body as a whole.

## References

- Abhilash, M. (2010) Potential applications of Nanoparticles. *International Journal of Pharma and Bio Sciences*, 1(1), 1-11.
- Agarwal, M., Murugan, M.S., Sharma, A., Rai, R., Kamboj, A., Sharma, H. and Roy, S.K. (2013) Nanoparticles and its Toxic Effects: A Review. *International Journal of Current Microbiology and Applied Sciences*, 2(10), 76-82.
- Allouche, J. (2013) Synthesis of Organic and Bioorganic Nanoparticles: An Overview of the Preparation Methods. In: Brayner, R., Fiévet, F. and Coradin T. (eds) *Nanomaterials: A Danger or a Promise?*. Springer, London.
- Arbain, R., Othman, M. and Palaniandy, S. (2011) Preparation of iron oxide nanoparticles by mechanical milling. *Minerals Engineering*, 24, 1-9.
- Armstead, A.L. and Li, B. (2016) Nanotoxicity: emerging concerns regarding nanomaterial safety and occupational hard metal (WC-Co) nanoparticle exposure. *International Journal of Nanomedicine*, 11, 6421- 6433.
- Arora, S., Rajwade, J.M. and Paknikar, K.M. (2012) Nanotoxicology and in vitro studies: The need of the hour. *Toxicology and Applied Pharmacology*, 258(2), 151–165.
- Barnett, J.B. and Brundage, K.M. (2010) Evaluating Macrophages in Immunotoxicity Testing. *Immunotoxicity Testing*, 598, 75-94.
- Bayati, M., Dai, J., Zambrana, A., Rees, C. and Fidalgo de Cortalezzi, M. (2017) Effect of water chemistry on the aggregation and photoluminescence behavior of carbon dots. *Journal of Environmental Sciences*, 1-13.



- Bertrand, N. and Leroux, J. (2012) The journey of a drug-carrier in the body: An anatomophysiological perspective. *Journal of Controlled Release*, 161, 152–163.
- Boraschi, D., Costantino, L. and Italiani, P. (2012) Interaction of nanoparticles with immunocompetent cells: nanosafety considerations. *Nanomedicine*, 7(1), 121-131.
- Boraschi, D., Italiani, P., Palomba, R., Decuzzi, P., Dusch, A., Fadeel, B. and Moghimi, S. M. (2017) Nanoparticles and innate immunity: new perspectives on host defence. *Seminars in Immunology*, 34, 33-51.
- Bryan, N.S. and Grisham, M.B. (2007) Methods to Detect Nitric Oxide and its Metabolites in Biological Samples. *Free Radical Biology and Medicine*, 43(5), 645- 657.
- Burda, C., Chen, X., Narayanan, R. and El-Sayed, M.A. (2005) Chemistry and Properties of Nanocrystals of Different Shapes. *Chemical Reviews*, 105 (4), 1025–1102.
- Cao, L., Wang, X., Mezziani, M. J., Lu, F., Wang, H., Luo, P.G., Lin, Y., Harruff, B. A., Veca, L.M., Murray, D., Xie, S. and Sun, Y. (2007) Carbon Dots for Multiphoton Bioimaging. *Journal of the American Chemical Society*, 123, 11318-11319.
- Chang, C. (2010) The immune effects of naturally occurring and synthetic nanoparticles. *Journal of Autoimmunity*, 34, J234- J246.
- Chen, D. H. and He, X.R. (2001) Synthesis of nickel ferrite nanoparticles by sol-gel method. *Materials Research Bulletin*, 36 (7-8), 1369-1377.
- Chen, H., Yu, S., Shin, D. and Yoo, J. (2010) Solvothermal Synthesis and Characterization of Chalcopyrite CuInSe<sub>2</sub> Nanoparticles. *Nanoscale Research Letters*, 5, 217–223.

Cho, M., Cho, W.S., Choi, M., Kim, S.J., Han, B.S., Kim, S.H., Kim, H.O., Sheen, Y.Y. and Jeong, J. (2009a) The impact of size on tissue distribution and elimination by single intravenous injection of silica nanoparticles. *Toxicology Letters*, 189(3), 177-83.

Cho, W., Cho, M., Jeong, J., Choi, M., Cho, H., Han, B.S., Kim, S.H., Kim, H.O., Lim, Y.T., Chung, B.H. and Jeong, J (2009b) Acute toxicity and pharmacokinetics of 13 nm-sized PEG-coated gold nanoparticles. *Toxicology and Applied Pharmacology*, 236(1), 16-24.

Davoren, M., Herzog, E., Casey, A., Cottineau, B., Chambers, G., Byrne, H.J. and Lyng, F.M. (2007) In vitro toxicity evaluation of single walled carbon nanotubes on human A549 lung cells. *Toxicology In Vitro: an International journal published in association with BIBRA*, 21(3), 438-48.

Descotes, J. (2005) Immunotoxicology: Role in the Safety Assessment of Drugs. *Drug Safety*, 28(2), 127-136.

De Jong, W.H., and Borm, P.J. (2008) Drug delivery and nanoparticles: Applications and hazards. *International Journal of Nanomedicine*, 3(2), 133–149.

De Jong, W.H. and Van Loveren, H. (2007) Screening of xenobiotics for direct immunotoxicity in an animal study. *Methods*, 41, 3–8.

Dimos, K. (2016) Carbon Quantum Dots: Surface Passivation and Functionalization. *Current Organic Chemistry*, 20, 682-695.

Dhawan, A. and Sharma, V. (2010) Toxicity assessment of nanomaterials: methods and challenges. *Analytical and Bioanalytical Chemistry*, 398, 589–605

Dobrovolskaia, M.A., Germolec, D.R. and Weaver, J.I. (2009) Evaluation of nanoparticle immunotoxicity. *Nature Nanotechnology*, 4, 411-414.

- Dobrovolskaia, M. A. and McNeil, S. E. (2007) Immunological properties of engineered nanomaterials. *Nature Nanotechnology*, 2(8), 469–478.
- Donaldson, K., Stone, V., Tran, C.L., Kreyling, W. and Borm, P.J.A. (2004) Nanotoxicology. *Occupational and Environmental Medicine*, 61, 727-727.
- Donner, E., Eriksson, E., Holten-Lützhøft, H., Scholes, L., Revitt, M. and Ledin, A. (2010) Identifying and Classifying the Sources and Uses of Xenobiotics in Urban Environments, Xenobiotics in the Urban Water Cycle: Mass Flows, Environmental Processes, Mitigation and Treatment Strategies. *Environmental Pollution*, 16, 27-50.
- Driscoll, K.E. (1994) Macrophage Inflammatory Proteins: Biology and Role in Pulmonary Inflammation. *Experimental Lung Research*, 20(6), 473-490.
- Dufour, J.H., Dziejman, M., Liu, M.T., Leung, J.H., Lane, T.E. and Luster, A.D. (2002) IFN- $\gamma$ -Inducible Protein 10 (IP-10; CXCL10)-Deficient Mice Reveal a Role for IP-10 in Effector T Cell Generation and Trafficking. *Journal of Immunology*, 168(7), 3195-3204.
- Duncan, T.V. (2011) Applications of nanotechnology in food packaging and food safety: Barrier materials, antimicrobials and sensors. *Journal of Colloid and Interface Science*, 363 (1), 1-24.
- Elsaesser, A. and Howard, C.V. (2012) Toxicology of nanoparticles. *Advanced Drug Delivery Reviews*, 6(2), 129-137.
- Eggleton, P. (2013) Hypersensitivity: Immune Complex Mediated (Type III). *ENCYCLOPEDIA OF LIFE SCIENCES*, 1-9.
- Esteves da Silva, J.C.G. and Gonçalves, H.M.R. (2011) Analytical and bioanalytical applications of carbon dots. *Trends in Analytical Chemistry*, 30, 1327–1336.

- Fu, P.P., Xia, Q., Hwang, H.M., Ray, P.C. and Yu, H. (2014) Mechanisms of nanotoxicity: generation of reactive oxygen species. *Journal of Food Drug Analysis*, 2(1), 64-75.
- Gao, Z., Shen, G., Zhao, X., Dong, N., Jia, P., Wu, J., Cui, D., Zhang, Y. and Wang, Y. (2013) Carbon dots: a safe nanoscale substance for the immunologic system of mice. *Nanoscale Research Letters*, 8(276), 1 -8.
- Gatoo, M.A., Naseem, S., Arfat, M.Y., Dar, A.M., Qasim, K. and Zubair, S. (2014) Physicochemical Properties of Nanomaterials: Implication in Associated Toxic Manifestations. *Biomed Research International*, 2014, 1-8.
- Germolec, D., Luebke, R., Rooney, A., Shipkowski, K., Vandebriel, R. and van Loveren, H. (2017) Immunotoxicology: A brief history, current status and strategies for future immunotoxicity assessment. *Current Opinion in Toxicology*, 5:55–59.
- Gruys, E., Toussaint, M.J.M., Niewold, T.A. and Koopmans, S.J. (2005) Acute phase reaction and acute phase proteins. *Journal of Zhejiang University Science B*, 6(11), 1045–1056.
- Havrdova, M., Hola, K., Skopalik, J., Tomankova, K., Petr, M., Cepe, K., Polakova, K., Tucek, J., Bourlinos, A. B. and Zboril, R. (2016) Toxicity of carbon dots – Effect of surface functionalization on the cell viability, reactive oxygen species generation and cell cycle. *Carbon*, 99, 238-248.
- He, X. and Hwang, H. (2016) Nanotechnology in food science: Functionality, applicability, and safety assessment. *JOURNAL OF FOOD AND DRUG ANALYSIS*, 24, 671- 681.
- Heiligtag, F.J. and Niederberger, M. (2013) The fascinating world of nanoparticle research. *Materials Today*, 16 (7/8), 262-271.

Hong, F., Ji, L., Zhou, Y. and Wang, L. (2017) Chronic nasal exposure to nanoparticulate TiO<sub>2</sub> causes pulmonary tumorigenesis in male mice. *Environmental Toxicology*, 32, 1651–1657.

Huang, X. and El-Sayed, M.A. (2010) Gold nanoparticles: Optical properties and implementations in cancer diagnosis and photothermal therapy. *Journal of Advanced Research*, 1, 13-28.

Janeway, C.A., Travers, P., Walport, M. and Shlomchik, M.J. (2001) *Immunobiology: The Immune System in Health and Disease* (5th edition). Garland Science, New York.

Jani, P., Halbert, G.W., Langridge, J. and Florence, A.T. (1990) Nanoparticle uptake by the rat gastrointestinal mucosa: quantitation and particle size dependency. *The Journal of Pharmacy and Pharmacology*, 42(12), 821-6.

Jylhä, M., Paavilainen, P., Lehtimäki, T., Goebeler, S., Karhunen, P.J., Hervonen, A. and Hurme, M. (2007) Interleukin-1 Receptor Antagonist, Interleukin-6, and C-Reactive Protein as Predictors of Mortality in Nonagenarians: The Vitality 90+ Study. *Journal of Gerontology: MEDICAL SCIENCES*, 62A (9), 1016–1021.

Kang, S.K., Lee, H.U., Kim, M., Park, S.Y., Chang, S., Park, J., Huh, Y.S., Lee, J., Yang, M., Lee, Y. and Park, H.G. (2015) In-vitro cytotoxicity assessment of carbon-nanodot-conjugated Fe-aminoclay (CD-FeAC) and its bio-imaging applications. *Journal of Nanobiotechnology*, 13:88 1-14.

Kelarakis, A. (2014) From highly graphitic to amorphous carbon dots: A critical review. *Materials Research Society*, 1 (2), 1-15.

Khan, I., Saeed, K. and Khan, I. (2017) Nanoparticles: Properties, applications and toxicities. *Arabian Journal of Chemistry*, 1-24.

Konig, R. (2011) Mechanisms of immune modulation by xenobiotics. *Encyclopedia of Environmental Health*, 3, 666-673.

Kononenko, V., Narat, M. and Drobne, D (2015) Nanoparticle interaction with the immune system. *Archives of Industrial Hygiene and Toxicology*, 66, 97-108.

Kreitinger, J.M., Beamer, C.A. and Shepherd, D.M. (2016) Environmental Immunology: Lessons Learned from Exposure to a Select Panel of Immunotoxicants. *The Journal of Immunology*, 196 (8), 3217-3225.

Kumar, R., Roy, I., Ohulchanskyy T.Y., Vathy, L.A., Bergey, E.J., Sajjad, M. and Prasad, P.N. (2010) In vivo biodistribution and clearance studies using multimodal organically modified silica nanoparticles. *ACS Nano*, 4(2), 699-708.

Kuricova, M., Tulinska, J., Liskova, A., Horvathova, M., Ilavska, S., Kovacikova, Z., Tatrai, E., Hurbankova, M., Cerna, S., Jahnova, E., Neubauerova, E., Wsolova, L., Wimmerova, S., Fuortes, L., Kyrtopoulos, S.A. and Dusinska, M. (2012) Immune System and Environmental Xenobiotics - The Effect of Selected Mineral Fibers and Particles on the Immune Response. *Recent Advances in Immunology to Target Cancer, Inflammation and Infections*, 335-380.

Li, Y., Guo, M., Zhan, M. and Wang, X. (2009) Hydrothermal synthesis and characterization of TiO<sub>2</sub> nanorod arrays on glass substrates. *Materials Research Bulletin*, 44, (6) 1232 – 1237.

Liang, H., Jin, C., Tang, Y., Wang, F., Ma, C. and Yang, Y. (2013) Cytotoxicity of silica nanoparticles on HaCaT cells. *Journal of Applied Toxicology*, 1-6.

Lin, M., Tan, J.P.Y., Boothroyd, C., Loh, K.P., Tok, E.S. and Foo, Y. (2006) Direct Observation of Single-Walled Carbon Nanotube Growth at the Atomistic Scale. *Nano Letters*, 6 (3), 449–452.

- Liu, Y., Liu, C.Y. and Zhang, Z.Y. (2012) Synthesis of highly luminescent graphitized carbon dots and the application in the Hg<sup>2+</sup> detection. *Applied Surface Science*, 263, 481–485.
- Liu, W.T. (2006) Nanoparticles and their biological and environmental applications. *Journal of Bioscience and Bioengineering*, 102 (1), 1-7.
- Liu, Y., Gao, Y., Zhang, L., Wang, T., Wang, J., Jiao, F., Li, W., Li, Y., Li, B., Chai, Z. Wu, G. and Chen, C. (2009) Potential health impact on mice after nasal instillation of nano-sized copper particles and their translocation in mice. *Journal of Nanoscience and Nanotechnology*, 9, 6335–6343.
- Luo, Y., Laning, J., Hayashi, M., Hancock, P.R., Rollins, B. and Dorf, M.E. (1994) Serologic analysis of the mouse beta chemokine JE/monocyte chemoattractant protein-1. *Journal of Immunology*, 153(8), 3708-3716.
- Maus, L., Dick, O., Bading, H., Spatz, J.P. and Fiammengo, R. (2010) Conjugation of Peptides to the Passivation Shell of Gold Nanoparticles for Targeting of Cell-Surface Receptors. *ACS Nano*, 4 (11), 6617–6628.
- Mehta, H.M., Malandra, M. and Corey, S.J. (2015) G-CSF and GM-CSF in Neutropenia. *Journal of Immunology*, 195(4), 1341-1349.
- Mills, A. and Hazafy, D. (2008) A solvent-based intelligence ink for oxygen. *The Analyst*, 133(2), 213-218.
- Mohanraj, V.J. and Chen, Y. (2006) Nanoparticles – A Review. *Tropical Journal of Pharmaceutical Research*, 5 (1), 561-573.

Mori, Y. (2015) Size-Selective Separation Techniques for Nanoparticles in Liquid. *KONA Powder and Particle Journal*, 32, 102-114.

Nabeshi, H., Yoshikawa, T., Matsuyama, K., Nakazato, Y., Arimori, A., Isobe, M., Tochigi, S., Kondoh, S., Hirai, T., Akase, T., Yamashita, T., Yamashita, K., Yoshida, T., Nagano, K., Abe, Y., Yoshioka, Y., Kamada, H., Imazawa, T., Itoh, N., Tsunoda, S. and Tsutsumi, Y. (2010) Size-dependent cytotoxic effects of amorphous silica nanoparticles on Langerhans cells. *Die Pharmazie*, 65(3), 199-201.

Napierska, D., Thomassen, L.C., Rabolli, V., Lison, D., Gonzalez, L., Kirsch-Volders, M., Martens, J.A. and Hoet, P.H. (2009) Size-dependent cytotoxicity of monodisperse silica nanoparticles in human endothelial cells. *Small (Weinheim an der Bergstrasse Germany)*, 5(7), 846-53.

National Research Council. (1992) *Biologic Markers in Immunotoxicology*. Washington, DC: The National Academies Press.

Oberdörster, G., Oberdörster, E. and Oberdörster, J. (2005) Nanotoxicology: An Emerging Discipline Evolving from Studies of Ultrafine Particles. *Environmental Health Perspectives*, 113 (7) 823-839.

Pal, S.L., Jana, U., Manna, P.L., Mohanta, G.P. and Manavalan, R. (2010) Nanoparticle: An overview of preparation and characterization. *Journal of Applied Pharmaceutical Science*, 01 (06), 228-234.

Pan, Y., Neuss, S., Leifert, A., Fischler, M., Wen, F., Simon, U., Schmid, G., Brandau, W. and Jahn-Dechen, W. (2007) Size-Dependent Cytotoxicity of Gold Nanoparticles. *Small*, 3 (11), 1941 – 1949.



Parameswaran, N. and Patial, S. (2010) Tumor necrosis factor- alpha signalling in macrophages. *Critical Reviews in Eukaryotic Gene Expression*, 20(2), 87-103.

Peng, H. and Travas-Sejdic, J. (2009) Simple Aqueous Solution Route to Luminescent Carbogenic Dots from Carbohydrates. *Chemistry of Materials Communication*, 21, 5563–5565.

Peters, R., Dam, G., Bouwmeester, H., Helsper, H., Allmaier, G., vd Kammer, F., Ramsch, R., Solans, C., Tomaniova, M., Hajslova, J. and Weigel, S. (2011) Identification and characterization of organic nanoparticles in food. *Trends in Analytical Chemistry*, 30 (1), 101-112.

Salata, O.V. (2004) Applications of nanoparticles in biology and medicine. *Journal of Nanobiotechnology*, 2, 1-6.

Santos, R.T. and Vieira, M.T. (2017) Assessment of airborne nanoparticles present in industry of aluminium surface treatments. *Journal of Occupational and Environmental Hygiene*, 14(3), D29-36.

Sayes, C.M. and Warheit, D.B. (2009) Characterization of nanomaterials for toxicity assessment. *Wiley Interdisciplinary Reviews: Nanomedicine and Nanobiotechnology*, 1(6):660-70.

Schmid, G. and Corain, B. (2003) Nanoparticulated Gold: Syntheses, Structures, Electronics, and Reactivities. *European Journal of Inorganic Chemistry*, 2003 (17), 3081–3098.

Schneider, M., Stracke, F., Hansen, S. and Schaefer, U.F. (2009) Nanoparticles and their interactions with the dermal barrier. *Dermato-Endocrinology*, 1(4), 197-206.

Shen, L., Zhang, L., Chen, M., Chen, X. and Wang, J. (2013) The production of pH-sensitive photoluminescent carbon nanoparticles by the carbonization of polyethylenimine and their use for bioimaging. *CARBON*, 55, 343 – 349.

Shevach, E.M. (2009) Immune Suppression. *Reference Module in Biomedical Sciences*, 3, 472–480.

Shi, Y., Liu, C.H., Roberts, A.I., Das, J., Xu, G., Ren, G., Zhang, Y., Zhang, L., Yuan, Z.R., Tan, H.S., Das, G. and Devadas, S. (2006) Granulocyte-macrophage colony-stimulating factor (GM-CSF) and T-cell responses: what we do and don't know. *Cell Research*, 16(2), 126-133.

Suk, J.S., Xu, Q., Kim, N., Hanes, J. and Ensigna, L.M. (2016) PEGylation as a strategy for improving nanoparticle-based drug and gene delivery. *Advanced Drug Delivery Reviews*, 99, 28–51.

Srinivasa, A., Rao, P.J., Selvam, G., Murthy, P.B. and Reddy, P.N. (2011) Acute inhalation toxicity of cerium oxide nanoparticles in rats. *Toxicology Letters*, 205(2), 105-115.

Sun, Y., Zhou, B., Lin, Y., Wang, W., Fernando, K.A.S., Pathak, P., Mezziani, J.M., Harruff, B. A., Wang, X., Wang, H., Luo, P.G., Yang, H., Kose, M.E., Bailin Chen, B., Veca, L.M. and Xie, S. (2006) Quantum-Sized Carbon Dots for Bright and Colorful Photoluminescence. *Journal of the American Chemical Society*, 128 (24), 7756–7757.

Sun, X. and Lei, Y. (2017) Fluorescent carbon dots and their sensing applications. *Trends in Analytical Chemistry*, 89, 163–180.

Sung, J. H., Ji, J. H., Yoon, J. U., Kim, D. S., Song, M. Y., Jeong, J., Han, B. S., Han, J. H., Chung, Y. H., Kim, J., Kim, T. S., Chang, H. K., Lee, E. J., Lee, J. H. and Yu, I. J. (2008) Lung function changes in Sprague-Dawley rats after prolonged inhalation exposure to silver nanoparticles. *Inhalation Toxicology*, 20(6), 567-574.

Swihart, M. T. (2003) Vapor-phase synthesis of nanoparticles. *Current Opinion in Colloid and Interface Science*, 8, 127–133.

Tao, S., Zhu, S., Feng, T., Xia, C., Song, Y. and Yang, B. (2017) The polymeric characteristics and photoluminescence mechanism in polymer carbon dots: A review. *Materials Today Chemistry*, 6, 13–25.

Tani, T., Mädler, L. and Pratsinis, S.E. (2002) Homogeneous ZnO Nanoparticles by Flame Spray Pyrolysis. *Journal of Nanoparticle Research*, 4 (4), 337–343.

Tien, D., Liao, C., Tseng, K. and Tsung, T. (2008) Discovery of ionic silver in silver nanoparticle suspension fabricated by arc discharge method. *Journal of Alloys and Compounds*, 463(1-2), 408-411.

Tsuji, T., Iryo, K., Watanabe, N. and Tsuji, M. (2002) Preparation of silver nanoparticles by laser ablation in solution: influence of laser wavelength on particle size. *Applied Surface Science*, 202 (1–2), 80-85.

Utekhina, A.Y. and Sergeev, G.B. (2011) Organic nanoparticles. *Russian Chemical Reviews*, 80 (3), 219- 233.

Vishwakarma, V., Samal, S.S., and Manoharan, N. (2010) Safety and Risk Associated with Nanoparticles - A Review. *Journal of Minerals & Materials Characterization & Engineering*, 9, (5), 455- 459.

Wang, K., Gao, Z., Gao, G., Wo, Y., Wang, Y., Shen, G. and Cui, D. (2013) Systematic safety evaluation on photoluminescent carbon dots. *Nanoscale Research Letters*, 8 (122), 1-9.

Wang, X., Qu, K., Ren, J. and Qu, X. (2011a) Microwave assisted one-step green synthesis of cell-permeable multicolour photoluminescent carbon dots without surface passivation reagents. *Journal of Materials Chemistry*, 211, 2445-2450.

Wang, Y., Anilkumar, P., Cao, L., Liu, J., Luo, P.G., Tackett, K.N., Sahu, S., Wang, P., Wang, X. and Sun, Y. (2011b) Carbon dots of different composition and surface functionalization: cytotoxicity issues relevant to fluorescence cell imaging. *Experimental Biology and Medicine*, 236, 1231–1238.

Wang, Y. and Hu, A. (2014) Carbon quantum dots: synthesis, properties and applications. *Journal of Materials Chemistry C*, 2, 6921-6939.

Warrington, R., Watson, W., Kim, H. L. and Antonetti, F. R. (2011) An introduction to immunology and immunopathology. *Allergy, Asthma & Clinical Immunology*, 7 (1), 1-8.

Weingart, J., Vabbilisetty, P. and Sun, X. (2013) Membrane mimetic surface functionalization of nanoparticles: Methods and applications. *Advances in Colloid and Interface Science*, 197-198, 68–84.

Weir, A., Westerhoff, P., Fabricius, L., Hristovski, K. and von Goetz, N. (2012) Titanium Dioxide Nanoparticles in Food and Personal Care Products. *Environmental Science & Technology*, 46, 2242–2250.

Wright, C., Iyer, A.K., Wang, L., Wu, N., Yakisich, J.S., Rojanasakul, Y. and Azad, N. (2017) Effects of titanium dioxide nanoparticles on human keratinocytes. *Drug and Chemical Toxicology*, 40(1), 90-100.

Xu, X., Ray, R., Gu, Y., Ploehn, H.J., Gearheart, L., Raker, K. and Scrivens, W.A. (2004) Electrophoretic Analysis and Purification of Fluorescent Single-Walled Carbon Nanotube Fragments. *Journal of the American Chemical Society*, 126 (40), 12736–12737.

Yadav, T. P., Yadav, R. M. and Singh, D. P. (2012) Mechanical Milling: a Top Down Approach for the Synthesis of Nanomaterials and Nanocomposites. *Nanoscience and Nanotechnology*, 2(3): 22-48.

Yang, S-T., Wang, X., Wang, H., Lu, F., Luo, P. G., Cao, L., Meziari, M.J., Liu, J-H., Liu, Y., Chen, M., Huang, Y. and Sun, Y.-P. (2009) Carbon Dots as Nontoxic and High-Performance Fluorescence Imaging Agents. *The Journal of Physical Chemistry C*, 113(42), 18110–18114.

Yang, W., Peters, J.I. and Williams, R.O. (2008) Inhaled nanoparticles- A current review. *International Journal of Pharmaceutics*, 356(1–2), 239-247.

Yildirimer, L., Thanh, N.T., Loizidou, M. and Seifalian, A.M. (2011) Toxicology and clinical potential of nanoparticles. *Nano Today*, 6(6), 585-607.

Yuan, Y., Guo B., Hao, L., Liu, N., Lin, Y., Guo, W., Li, X. and Gu, B. (2017) Doxorubicin-loaded environmentally friendly carbon dots as a novel drug delivery system for nucleus targeted cancer therapy. *Colloids and Surfaces B: Biointerfaces*, 159, 349-359.

Zhang, J. and Yu, S. (2015) Carbon dots: large-scale synthesis, sensing and bioimaging. *Materials Today*, 00(00), 1-12.

Zhang, T., Tang, M., Kong, L., Li, H., Zhang, T., Zhang, S., Xue, Y. and Pu, Y. (2012) Comparison of cytotoxic and inflammatory responses of pristine and functionalized multi-walled carbon

nanotubes in RAW 264.7 mouse macrophages. *Journal of Hazardous Materials*, 219–220:203-212.

Zhu, S., Song, Y., Zhao, X., Shao, J., Zhang, J. and Yang, B. (2015) The photoluminescence mechanism in carbon dots (graphene quantum dots, carbon nanodots, and polymer dots): current state and future perspective, *Nano Research*, 8, 355–381.

Zoroddu, M.A., Medici, S., Ledda, A., Nurchi, V.M., Lachowicz, J.I. and Peana, M. (2014) Toxicity of Nanoparticles. *Current Medicinal Chemistry*, 21, 3837-385.